This article has been accepted for publication in a future issue of this journal, but has not been fully edited. Content may change prior to final publication. Citation information: DOI 10.1109/TNNLS.2025.3579254,

New WTOD Protocol-Based Fault Detection Filter Design for Interval Type-2 Fuzzy Systems via an Adaptive Differential Evolution Algorithm

Wei Qian, *Senior Member, IEEE*, Yanmin Wu, and Zidong Wang, *Fellow, IEEE*

***Abstract*—This article is concerned with the design problem of an H_∞ optimal fault detection (FD) filter for networked interval type-2 (IT2) fuzzy systems that are subjected to stochastic cyberattacks. To effectively reduce the utilization of constrained network resources, a new dynamically adjusted event-triggered weighted try-once-discard (DAET-WTOD) protocol is developed, in which two adaptive rules are constructed based on the measured output and the probability of denial-of-service (DoS) attacks. Furthermore, a fuzzy switched-like FD filter is designed with the purpose of detecting system fault signals, while simultaneously considering the DAET-WTOD protocol and stochastic cyberattacks. Subsequently, by utilizing an imperfect premise matching (IPM) scheme, an opposition-based learning adaptive differential evolution algorithm is proposed to deal with the networked IT2 fuzzy systems. This algorithm is capable of iteratively searching the membership function values of the fuzzy filter in real time, thereby achieving improved H_∞ performance. Finally, some simulation results are provided to verify the feasibility and advantages of the proposed H_∞ optimal FD technique.**

***Index Terms*—Adaptive differential evolution (ADE) algorithm, fault detection (FD), interval type-2 (IT2) fuzzy systems, opposition-based learning, stochastic cyberattacks, weighted try-once-discard (WTOD) protocol.**

Nomenclature

T–S	Takagi-Sugeno.
FD	Fault detection.
IT2	Interval type-2.
MFs	Membership functions.
IPM	Imperfect premise matching.
ADE	Adaptive differential evolution.
WTOD	Weighted try-once-discard.
DAET-WTOD	Dynamically adjusted event-triggered weighted try-once-discard.

I. Introduction

DUE to the critical importance of FD for the safe operation and maintenance of industrial systems, the field of FD in nonlinear systems has received widespread attention. As an effective tool for modeling nonlinear systems [17], the T-S fuzzy method has been applied in various fields [3], [7], [8], [28], [31], [34]. Considering the uncertain parameters of nonlinear plants, the IT2 T-S fuzzy modeling method has been proposed in [14], [44], and [50]. Several significant FD-related issues have been explored for T-S fuzzy systems and many excellent results have been reported in the literature. For instance, to detect system faults, a sequence of iterative proportional-integral observers has been developed for discrete-time T-S fuzzy systems in [29]. In line with the IT2 T-S fuzzy model, the FD filter design issue has been addressed in [46] for a class of nonlinear systems with sensor saturation. Taking finite frequency performance indices into account, a new FD strategy has been developed in [16]. Furthermore, the advancement of information technology and wireless communication technology has significantly accelerated the development of networked control systems (NCSs). Recently, considering the wireless communication technology, the network-based FD problem has emerged as a prominent research focus.

Although NCSs offer several unique advantages, the introduction of wireless network communication also presents new challenges. In real-world network communication, the bandwidth of communication channels is limited, and traditional time-triggered mechanisms may lead to network congestion, resulting in slower system response and potential instability. To address this issue, the event-triggered (ET) communication scheme [24], [51] has been proposed by designing an ET condition, which reduces unnecessary data transmission. Several significant results related to ET-based FD strategies have been reported. For instance, an event-driven FD technique, considering the parameter uncertainty of the plant, has been explored in [25] for networked fuzzy systems. Furthermore, an adaptive ET-based reduced-order FD filter has been developed in [26] for a class of T-S fuzzy systems with complex communication channels.

Compared to ET communication mechanisms, data scheduling protocols allow only one sensor to transmit data to the communication channel at a time, thereby reducing the communication burden [38]. Generally, these data scheduling protocols include round-robin protocol [37], stochastic communication protocol [4], [41], WTOD protocol [15], [19], and FlexRay protocol [20]. Due to its high efficiency, the WTOD protocol has garnered much attention from control and

Received 25 October 2024; revised 24 April 2025; accepted 3 June 2025. This work was supported in part by the National Natural Science Foundation of China under Grant 62373137. *(Corresponding author: Wei Qian.)*

Wei Qian and Yanmin Wu are with the School of Electrical Engineering and Automation, Henan Polytechnic University, Jiaozuo 454000, China (e-mail: qwei@hpu.edu.cn; wuyanmin188@163.com).

Zidong Wang is with the Department of Computer Science, Brunel University London, UB8 3PH Uxbridge, U.K. (e-mail: Zidong.Wang@brunel.ac.uk).

This article has been accepted for publication in a future issue of this journal, but has not been fully edited. Content may change prior to final publication. Citation information: DOI 10.1109/TNNLS.2025.3579254, IEEE TRANSACTIONS ON NEURAL NETWORKS AND LEARNING SYSTEMS

signal processing communities. For example, a nonfragile set-membership filter has been designed in [13] for 2-D systems under communication constraints. Furthermore, slow and fast controllers have been designed using the asynchronous WTOD protocol to ensure asymptotic stability for networked singularly perturbed systems in [11]. However, WTOD's inability to handle significant signal fluctuations and the potential waste of resources (when fluctuations are minimal) highlight the need for a new WTOD protocol, which can then be applied to IT2 fuzzy FD systems.

On the other hand, parallel distribution compensation (PDC) methods [43] have typically been employed for designing fuzzy controllers. However, PDC technology requires that the MFs of the controller and the system be identical, which can lead to significant conservatism. To address this issue, the IPM strategy has been introduced. In [47], an IPM-based fuzzy state feedback controller has been developed to ensure that IT2 fuzzy semi-Markov systems remain finite-time stochastically stable. Furthermore, an observer-based repetitive controller design scheme using the IPM technique has been investigated in [33] for networked nonlinear systems subjected to multiple network attacks. Notably, the controller's MFs can be selected freely within a limited region, and this selection process is typically based on the designer's intuition and experience, which may ensure system stability but not necessarily achieve the desired system performance.

To attain better H_∞ performance, a novel MF online iteration strategy has been proposed in [23] and [48] to optimize the controller MFs based on the IPM approach for T-S fuzzy systems. This MF online learning algorithm has also been applied to improve driving comfort levels in fuzzy vehicle suspension systems in [48]. However, it is well-known that the gradient descent approach used in MF online learning algorithms [48] is highly sensitive to initial parameter values, which may result in different local optimal solutions depending on the initial values chosen. To overcome this challenge, a new MF online learning method incorporating the differential evolution (DE) algorithm has been proposed in [49] to achieve the desired H_∞ performance. Note that the conventional DE algorithm has limitations such as premature convergence and low search capability. Moreover, few studies have addressed the complex problem of H_∞ performance optimization for IT2 fuzzy FD systems under stochastic cyberattacks and data scheduling protocols. Therefore, designing a new FD scheme to address these challenges is another key motivation of this article.

This article explores a new H_∞ optimal FD scheme for networked IT2 fuzzy systems subjected to stochastic cyberattacks under a new WTOD protocol. The main contributions are outlined as follows.

1) To manage the data transmission of distributed sensors more efficiently, a DAET-WTOD protocol is proposed. Unlike the existing WTOD protocols [11], [19], the DAET-WTOD protocol integrates both an adaptive ET mechanism and the WTOD protocol. This integration includes two time-varying adaptive rules that regulate thresholds based on the system's dynamic information.
2) A fuzzy switched-like FD filter with asynchronous MFs is designed, considering both the DAET-WTOD protocol and stochastic cyberattacks. This filter effectively diagnoses system faults in networked IT2 fuzzy FD systems.
3) Building on the IPM technique, a new MF online optimization approach utilizing an opposition-based learning ADE algorithm is introduced for networked IT2 fuzzy FD systems. Through this MF optimization technique, better H_∞ performance is achieved by finding the optimal fuzzy FD filter MFs in real time.

The structure of this article is organized as follows. Section II presents the problem formulation, while Section III outlines the main results. Sections IV and V cover the simulation verification and the conclusion, respectively.

In addition, to better understand the abbreviations used in this article, the Nomenclature regarding the main terminological abbreviations is provided.

II. Problem Description and Preliminaries

A. Networked IT2 Fuzzy Model

The considered nonlinear plant is described by the IT2 fuzzy model equipped with $\hbar$ rules.

Plant Rule t: **IF** $O_1(\mathbf{x}(\mathbf{k}))$ is Ψ_1^t, AND $\cdots$ AND$O_\hbar(\mathbf{x}(\mathbf{k}))$ is $\Psi_\hbar^t$, **THEN**

$$\begin{aligned}\mathbf{x}(\mathbf{k}+1) &= A_t\mathbf{x}(\mathbf{k}) + E_t\mathbf{w}(\mathbf{k}) + E_{ft}\mathbf{f}(\mathbf{k})\\ \mathbf{y}(\mathbf{k}) &= C_t\mathbf{x}(\mathbf{k})\end{aligned} \quad (1)$$

where $O_a(\mathbf{x}(\mathbf{k}))(a = 1, 2, \ldots, \hbar)$ and $\Psi_a^t(t = 1, 2, \ldots, \hbar)$ are, respectively, the premise variables and the fuzzy sets, in which $\hbar$ and $\hbar$ stand for the number of IF-THEN rules and premise variables, respectively. $\mathbf{x}(\mathbf{k}) \in \mathbb{R}^{\mathbf{n_x}}$ denotes the system state vector. $\mathbf{y}(\mathbf{k}) \in \mathbb{R}^{\mathbf{n_y}}$ represents the measured output vector. $\mathbf{w}(\mathbf{k}) \in \mathbb{R}^{\mathbf{n_w}}$ and $\mathbf{f}(\mathbf{k}) \in \mathbb{R}^{\mathbf{n_f}}$ stand for the external perturbation satisfying $L_2[0, \infty)$ and the fault signal, respectively. A_t, E_t, E_{ft}, and C_t stand for known system matrices. The activation intensity of the tth fuzzy rule is described as $\mathcal{E}_t(\mathbf{x}(\mathbf{k})) = [\underline{\varepsilon}_t(\mathbf{x}(\mathbf{k})), \bar{\varepsilon}_t(\mathbf{x}(\mathbf{k}))]$, where $\underline{\varepsilon}_t(\mathbf{x}(\mathbf{k})) = \prod_{a=1}^{\hbar} \underline{\epsilon}_{\Psi_a^t}(O_a(\mathbf{x}(\mathbf{k}))) \geq 0, \bar{\varepsilon}_t(\mathbf{x}(\mathbf{k})) = \prod_{a=1}^{\hbar} \bar{\epsilon}_{\Psi_a^t}(O_a(\mathbf{x}(\mathbf{k}))) \geq 0$. $\underline{\varepsilon}_t(\mathbf{x}(\mathbf{k}))$ and $\bar{\varepsilon}_t(\mathbf{x}(\mathbf{k}))$ are the lower and upper MFs (LUMFs) contenting $\bar{\varepsilon}_t(\mathbf{x}(\mathbf{k})) \geq \underline{\varepsilon}_t(\mathbf{x}(\mathbf{k}))$. The lower and upper membership grades (LUMGs) are represented by $\underline{\epsilon}_{\Psi_a^t}(O_a(\mathbf{x}(\mathbf{k})))$ and $\bar{\epsilon}_{\Psi_a^t}(O_a(\mathbf{x}(\mathbf{k})))$, in which $\bar{\epsilon}_{\Psi_a^t}(O_a(\mathbf{x}(\mathbf{k}))) \geq \underline{\epsilon}_{\Psi_a^t}(O_a(\mathbf{x}(\mathbf{k})))$.

Similar to [42], the IT2 fuzzy model is deduced as

$$\begin{aligned}\mathbf{x}(\mathbf{k}) &= \sum_{t=1}^{\hbar} g_t(\mathbf{x}(\mathbf{k}))\left[A_t\mathbf{x}(\mathbf{k}) + E_t\mathbf{w}(\mathbf{k}) + E_{ft}\mathbf{f}(\mathbf{k})\right]\\ \mathbf{y}(\mathbf{k}) &= \sum_{t=1}^{\hbar} g_t(\mathbf{x}(\mathbf{k}))\left[C_t\mathbf{x}(\mathbf{k})\right]\end{aligned} \quad (2)$$

where

$$g_t(\mathbf{x}(\mathbf{k})) = \frac{\hat{g}_t(\mathbf{x}(\mathbf{k}))}{\sum_{t=1}^{\hbar} \hat{g}_t(\mathbf{x}(\mathbf{k}))}, \quad \sum_{t=1}^{\hbar} g_t(\mathbf{x}(\mathbf{k})) = 1$$

$$\hat{g}_t(\mathbf{x}(\mathbf{k})) = \underline{H}_t(\mathbf{x}(\mathbf{k}))\underline{\varepsilon}_t(\mathbf{x}(\mathbf{k})) + \bar{H}_t(\mathbf{x}(\mathbf{k}))\bar{\varepsilon}_t(\mathbf{x}(\mathbf{k})).$$

The normalized membership can be represented by $g_t(\mathbf{x}(\mathbf{k}))$. $\underline{H}_t(\mathbf{x}(\mathbf{k})) \in [0, 1]$ and $\bar{H}_t(\mathbf{x}(\mathbf{k})) \in [0, 1]$ are

This article has been accepted for publication in a future issue of this journal, but has not been fully edited. Content may change prior to final publication.
Citation information: DOI 10.1109/TNNLS.2025.3579254, IEEE Transactions on Neural Networks and Learning Systems

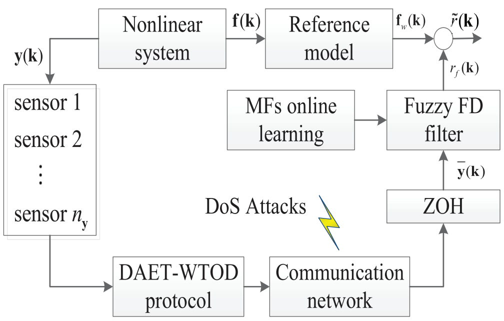

Fig. 1. Networked FD system with DAET-WTOD protocol.

nonlinear weighting functions (NWFs) that satisfy $\underline{H}_\iota(\mathbf{x}(\mathbf{k})) + \bar{H}_\iota(\mathbf{x}(\mathbf{k})) = 1$.

B. Probability-Dependent DAET-WTOD Protocol

As shown in Fig. 1, the measured output $\mathbf{y}(\mathbf{k})$ is transmitted via a wireless network communication link and scheduled according to a new data transmission strategy. Suppose that there are $\mathbf{n_y}$ sensor nodes. In addition, $\mathbf{y}(\mathbf{k}) = [\mathbf{y}_1^T(\mathbf{k}), \mathbf{y}_2^T(\mathbf{k}), \ldots, \mathbf{y}_{\mathbf{n_y}}^T(\mathbf{k})]^T$, in which the sampling signal of the ιth sensor can be represented by $\mathbf{y}_\iota(\mathbf{k})$ ($\iota = 1, 2, \ldots, \mathbf{n_y}$). For the ιth sensor node, the following function is devised:

$$\mathbf{u}_\iota(\mathbf{k}) = \left(\mathbf{y}_\iota\left(\ell^\iota_{\mathrm{p}-1}\right) - \mathbf{y}_\iota(\mathbf{k})\right)^T \phi_\iota \left(\mathbf{y}_\iota\left(\ell^\iota_{\mathrm{p}-1}\right) - \mathbf{y}_\iota(\mathbf{k})\right) \tag{3}$$

in which $\mathbf{y}_\iota(\ell^\iota_{\mathrm{p}-1})$ denotes the latest triggered output data of the ιth sensor node. $\phi_\iota > 0$ stands for the given weighting matrix. Therefore, $\mathbf{u}_\iota(\mathbf{k})$ represents the deviation between the current sampling data and the previously transmitted packet $\mathbf{y}_\iota(\ell^\iota_{\mathrm{p}-1})$ for the ιth sensor node. Based upon the traditional WTOD protocol [19], the index of the sensor node that is selected to trigger measured data at the present moment $\mathbf{k}$ can be determined by the following condition:

$$\Upsilon(\mathbf{k}) = \arg\max_{1\le\iota\le\mathbf{n_y}} \mathbf{u}_\iota(\mathbf{k}) \tag{4}$$

where $\Upsilon(\mathbf{k}) \in \{1, 2, \ldots, \mathbf{n_y}\}$. It is clear that only one sensor node can be selected to transmit the measured output data to the wireless communication network at a time. Unlike the existing WTOD protocol [19], a novel packet transmission scheme is introduced that simultaneously integrates a probability-dependent adaptive ET mechanism with the WTOD protocol to more effectively manage the transmission of measured packets among multiple sensor nodes. Two time-varying threshold functions, $\sigma_{\max}(\mathbf{k})$ and $\sigma_{\min}(\mathbf{k})$, are provided, where $\sigma_{\max}(\mathbf{k}) \in [\underline{\sigma}_{\max}, \overline{\sigma}_{\max}]$ and $\sigma_{\min}(\mathbf{k}) \in [\underline{\sigma}_{\min}, \overline{\sigma}_{\min}]$. In addition, to construct the new data transmission protocol, a positive parameter λ_ι is given, where $\iota \in \{1, 2, \ldots, \mathbf{n_y}\}$. As a result, the following three scenarios can be considered.

1) Case I: If there exists $\mathbf{u}_\iota(\mathbf{k}) \ge \sigma_{\max}(\mathbf{k})\mathbf{y}_\iota(\mathbf{k})^T\lambda_\iota\mathbf{y}_\iota(\mathbf{k})$, all sensor nodes can release the current sampling data at instant $\mathbf{k}$. The upper bound time-varying threshold function is provided as follows:

$$\sigma_{\max}(\mathbf{k}+1) = \sigma_{\max}(\mathbf{k}) + \begin{cases} \left(\sigma_{\max}(\mathbf{k}) - \underline{\sigma}_{\max}\right)\tanh\left(-\beta_1\left(1+\bar{\theta}\right)\|e(\mathbf{k})\|^2\right), & \text{if } \zeta(\mathbf{k}) \le 0 \\ \left(\overline{\sigma}_{\max} - \sigma_{\max}(\mathbf{k})\right)\tanh\left(\beta_1\left(1-\bar{\theta}\right)\|e(\mathbf{k})\|^2\right), & \text{if } \zeta(\mathbf{k}) > 0 \end{cases} \tag{5}$$

where $0 < \underline{\sigma}_{\max} \le \overline{\sigma}_{\max}$. β_1 stands for a positive constant. $e(\mathbf{k}) = \mathbf{y}(\ell_{\mathrm{p}}) - \mathbf{y}(\mathbf{k})$. $\zeta(\mathbf{k}) = \|\mathbf{y}(\ell_{\mathrm{p}})\| - \|\mathbf{y}(\mathbf{k})\|$. $\bar{\theta}$ denotes the probability of denial-of-service (DoS) attacks, which will be described in the following.

2) Case II: If the condition in *Case I* is not met but there exist any $\mathbf{u}_\iota(\mathbf{k}) \ge \sigma_{\min}(\mathbf{k})\mathbf{y}_\iota(\mathbf{k})^T\lambda_\iota\mathbf{y}_\iota(\mathbf{k})$, the packet of the ιth sensor node is transmitted to the network at instant $\mathbf{k}$. The lower bound time-varying threshold function is given as follows:

$$\sigma_{\min}(\mathbf{k}+1) = \sigma_{\min}(\mathbf{k}) + \begin{cases} \left(\sigma_{\min}(\mathbf{k}) - \underline{\sigma}_{\min}\right)\tanh\left(-\beta_2\left(1+\bar{\theta}\right)\|e(\mathbf{k})\|^2\right), & \text{if } \zeta(\mathbf{k}) \le 0 \\ \left(\overline{\sigma}_{\min} - \sigma_{\min}(\mathbf{k})\right)\tanh\left(\beta_2\left(1-\bar{\theta}\right)\|e(\mathbf{k})\|^2\right), & \text{if } \zeta(\mathbf{k}) > 0 \end{cases} \tag{6}$$

where $0 < \underline{\sigma}_{\min} \le \overline{\sigma}_{\min}$. β_2 is a positive constant.

3) Case III: If there is no $\mathbf{u}_\iota(\mathbf{k})$ that satisfies either *Case I* or *Case II*, but all measured data content $\mathbf{u}_\iota(\mathbf{k}) < \sigma_{\min}(\mathbf{k})\mathbf{y}_\iota(\mathbf{k})^T\lambda_\iota\mathbf{y}_\iota(\mathbf{k})$, then no measured packets are released to the network at instant $\mathbf{k}$.

In the following discussion, S_1–S_3 are defined to represent the moments that satisfy *Cases I – III*, respectively. Subsequently, the release of the measured output $\mathbf{y}(\mathbf{k})$ can be analyzed according to these three different scenarios.

Case I: For $\mathbf{k} \in \mathbf{S}_1$, there exists $\mathbf{u}_\iota(\mathbf{k})$ contenting

$$\mathbf{u}_\iota(\mathbf{k}) \ge \sigma_{\max}(\mathbf{k})\mathbf{y}_\iota(\mathbf{k})^T\lambda_\iota\mathbf{y}_\iota(\mathbf{k}). \tag{7}$$

Considering the designed probability-dependent DAET-WTOD protocol and the stochastic DoS attack caused by malicious network attacks under zero-order holder (ZOH) strategy, the transmission rule of the signal $\mathbf{y}_\iota(\ell^\iota_{\mathrm{p}})$ can be represented by

$$\mathbf{y}_\iota\left(\ell^\iota_{\mathrm{p}}\right) = \begin{cases} \left(1-\theta(\mathbf{k})\right)\mathbf{y}_\iota(\mathbf{k}), & \text{if } \mathbf{y}_\iota(\mathbf{k}) \text{satisfies (7)} \\ \mathbf{y}_\iota\left(\ell^\iota_{\mathrm{p}-1}\right), & \text{else} \end{cases} \tag{8}$$

where $\mathbf{y}_\iota(\ell^\iota_{\mathrm{p}})$ stands for the sampling packet received by the filter from the ιth sensor node. $\theta(\mathbf{k})$ denotes a random variable that satisfies the following Bernoulli process:

$$\mathrm{Prob}\{\theta(\mathbf{k}) = 0\} = 1 - \bar{\theta}, \quad \mathrm{Prob}\{\theta(\mathbf{k}) = 1\} = \bar{\theta} \tag{9}$$

in which $\bar{\theta} \in [0, 1]$ is a known parameter. If the measured signal $\mathbf{y}_\iota(\mathbf{k})$ satisfies (7) and $\theta(\mathbf{k}) = 0$, it indicates that there is no DoS attack on the ιth sensor node at the current moment, allowing the filter to receive the measured packet $\mathbf{y}_\iota(\mathbf{k})$. Conversely, $\theta(\mathbf{k}) = 1$ signifies that the ιth sensor node is under attack by malicious hackers.

Define $e_\iota(\mathbf{k}) = \mathbf{y}_\iota(\ell_{\rm p}^\iota) - \mathbf{y}_\iota(\mathbf{k}), (1, 2, \ldots, \mathbf{n_y})$ and $e(\mathbf{k}) = [e_1^T(\mathbf{k}), e_2^T(\mathbf{k}), \ldots, e_{\mathbf{n_y}}^T(\mathbf{k})]^T$. When the measured signal $\mathbf{y}_\iota(\mathbf{k})$ satisfies the condition (7), $e_\iota(\mathbf{k}) = (1 - \theta(\mathbf{k}))(\mathbf{y}_\iota(\ell_{\rm p}^\iota) - \mathbf{y}_\iota(\mathbf{k}))$, and $e_\iota^T(\mathbf{k})\phi_\iota e_\iota(\mathbf{k})$ is 0 or $\mathbf{y}_\iota(\mathbf{k})^T\phi_\iota\mathbf{y}_\iota(\mathbf{k})$; therefore, one has $\sigma_{\max}(\mathbf{k})\mathbf{y}_\iota(\mathbf{k})^T\lambda_\iota\mathbf{y}_\iota(\mathbf{k}) \geq e_\iota^T(\mathbf{k})\phi_\iota e_\iota(\mathbf{k})$, in which $\sigma_{\max}(\mathbf{k})\lambda_\iota \geq \phi_\iota$. In the case that the measured signal $\mathbf{y}_\iota(\mathbf{k})$ does not satisfy the condition (7), one derives $\mathbf{y}_\iota(\ell_{\rm p}^\iota) = \mathbf{y}_\iota(\ell_{\rm p-1}^\iota)$, then $e_\iota^T(\mathbf{k})\phi_\iota e_\iota(\mathbf{k}) = \mathbf{u}_\iota(\mathbf{k})$, which signifies that $\sigma_{\max}(\mathbf{k})\mathbf{y}_\iota(\mathbf{k})^T\lambda_\iota\mathbf{y}_\iota(\mathbf{k}) > e_\iota^T(\mathbf{k})\phi_\iota e_\iota(\mathbf{k})$. Moreover, one derives

$$\sum_{\iota=1}^{\mathbf{n_y}} \left[\sigma_{\max}(\mathbf{k})\,\mathbf{y}_\iota(\mathbf{k})^T\lambda_\iota\mathbf{y}_\iota(\mathbf{k}) - e_\iota^T(\mathbf{k})\,\phi_\iota e_\iota(\mathbf{k})\right] \geq 0. \tag{10}$$

In addition, (10) holds if

$$\sigma_{\max}(\mathbf{k})\mathbf{y}(\mathbf{k})^T\Lambda\mathbf{y}(\mathbf{k}) - e^T(\mathbf{k})Fe(\mathbf{k}) \geq 0 \tag{11}$$

where $\Lambda = \mathrm{diag}\{\lambda_1, \lambda_2, \ldots, \lambda_{\mathbf{n_y}}\}$ and $F = \mathrm{diag}\{\phi_1, \phi_2, \ldots, \phi_{\mathbf{n_y}}\}$.

Case II: For $\mathbf{k} \in \mathbf{S}_2$, there exists $\mathbf{u}_\iota(\mathbf{k})$ contenting

$$\mathbf{u}_\iota(\mathbf{k}) \geq \sigma_{\min}(\mathbf{k})\mathbf{y}_\iota(\mathbf{k})^T\lambda_\iota\mathbf{y}_\iota(\mathbf{k}). \tag{12}$$

In this case, based on the (4), the corresponding sensor node $\Upsilon(\mathbf{k})$ is selected. The input signal $\bar{\mathbf{y}}_\iota(\mathbf{k})$ obtained by the filter can be characterized in detail via

$$\bar{\mathbf{y}}_\iota(\mathbf{k}) = \begin{cases}(1 - \theta(\mathbf{k}))\,\mathbf{y}_\iota(\mathbf{k}), & \text{if } \iota = \Upsilon(\mathbf{k}) \\ \bar{\mathbf{y}}_\iota(\mathbf{k}-1), & \text{otherwise.}\end{cases} \tag{13}$$

Set $\bar{\mathbf{y}}(\mathbf{k}) = [\bar{\mathbf{y}}_1^T(\mathbf{k}), \bar{\mathbf{y}}_2^T(\mathbf{k}), \ldots, \bar{\mathbf{y}}_{\mathbf{n_y}}^T(\mathbf{k})]^T$. Therefore, the following formula is obtained:

$$\bar{\mathbf{y}}(\mathbf{k}) = (1 - \theta(\mathbf{k}))\Psi_{\Upsilon(\mathbf{k})}\mathbf{y}(\mathbf{k}) + \tilde{\Psi}_{\Upsilon(\mathbf{k})}\bar{\mathbf{y}}(\mathbf{k}-1) \tag{14}$$

where $\bar{\mathbf{y}}(\mathbf{k}) \in \mathbb{R}^{\mathbf{n_y}}$ represents the input signal of the filter. $\Psi_{\Upsilon(\mathbf{k})} = \mathrm{diag}\{\delta(\Upsilon(\mathbf{k}) - 1), \ldots, \delta(\Upsilon(\mathbf{k}) - \mathbf{n_y})\}.\tilde{\Psi}_{\Upsilon(\mathbf{k})} = I - \Psi_{\Upsilon(\mathbf{k})}$. $\delta(\cdot) \in \{0, 1\}$ stands for the Kronecker delta function.

Case III: For $\mathbf{k} \in \mathbf{S}_3$, all $\mathbf{u}_r(\mathbf{k})$ satisfy

$$\mathbf{u}_\iota(\mathbf{k}) < \sigma_{\min}(\mathbf{k})\mathbf{y}_\iota(\mathbf{k})^T\lambda_\iota\mathbf{y}_\iota(\mathbf{k}). \tag{15}$$

When (15) is satisfied, based upon the input signal retention mechanism, we have

$$\bar{\mathbf{y}}_\iota(\mathbf{k}) = \bar{\mathbf{y}}_\iota(\mathbf{k}-1). \tag{16}$$

For all $\mathbf{y}_\iota(\mathbf{k})$, by using (15) and (16), it is deduced that $\sigma_{\min}(\mathbf{k})\mathbf{y}_\iota^T(\mathbf{k})\lambda_\iota\mathbf{y}_\iota(\mathbf{k}) > (\bar{\mathbf{y}}_\iota(\mathbf{k}-1) - \mathbf{y}_\iota(\mathbf{k}))^T\phi_\iota(\bar{\mathbf{y}}_\iota(\mathbf{k}-1) - \mathbf{y}_\iota(\mathbf{k}))$, that is

$$\sum_{\iota=1}^{\mathbf{n_y}} \left[\sigma_{\min}(k)\,\mathbf{y}_\iota(\mathbf{k})^T\lambda_\iota\mathbf{y}_\iota(\mathbf{k}) - e_\iota^T(\mathbf{k})\,\phi_\iota e_r(\mathbf{k})\right] > 0 \tag{17}$$

and therefore,

$$\sigma_{\min}(\mathbf{k})\mathbf{y}^T(\mathbf{k})\Lambda\mathbf{y}(\mathbf{k}) - e^T(\mathbf{k})Fe(\mathbf{k}) \geq 0. \tag{18}$$

Remark 1: The new DAET-WTOD protocol is designed by leveraging the characteristics of the adaptive ET mechanism and the principles of the WTOD protocol. This design allows for dynamic management of the number of triggering packet sensors in distributed sensor networks. Within the DAET-WTOD protocol, two adaptive rules are formulated to adjust the ET thresholds $\sigma_{\max}(\mathbf{k})$ and $\sigma_{\min}(\mathbf{k})$ based on real-time system dynamics and the probability of DoS attacks. Given the constraints of limited communication bandwidth, the proposed DAET-WTOD protocol is more effective in conserving communication resources while ensuring FD performance under stochastic cyberattacks.

Remark 2: Based on the transformation tendency $\zeta(\mathbf{k})$, the adaptive rules (5) and (6) can dynamically adjust the ET thresholds $\sigma_{\max}(\mathbf{k})$ and $\sigma_{\min}(\mathbf{k})$. When $\zeta(\mathbf{k}) > 0$, the ET threshold $\sigma_{\max}(\mathbf{k})$ increases toward $\overline{\sigma}_{\max}$; otherwise, it decreases toward $\underline{\sigma}_{\max}$. The adaptive adjustment of the ET threshold $\sigma_{\min}(\mathbf{k})$ follows the same principle as $\sigma_{\max}(\mathbf{k})$. Unlike the existing adaptive rule [40], which only provides a lower bound, this approach defines two bounded ranges, $[\underline{\sigma}_{\max}, \overline{\sigma}_{\max}]$ and $[\underline{\sigma}_{\min}, \overline{\sigma}_{\min}]$. These bounded ranges prevent difficulties in data transmission due to the unbounded continuous increase of ET thresholds and address the problem of frequent data triggering caused by overly small ET thresholds.

Remark 3: Unlike the normal WTOD protocol [11], which only allows one sensor to transmit data to the network, the proposed DAET-WTOD protocol categorizes sensor data into three scenarios to manage data transmission based on the size of data fluctuations. This approach allows for more efficient use of limited communication resources, further conserving bandwidth while ensuring effective data transmission.

C. Asynchronous Mf-Based FD Filter

Under the IPM strategy, the FD filter subjected to asynchronous MFs can be devised as follows.

Filter Rule h: **IF** $\varphi_1(\mathbf{x}_f(\mathbf{k}))$ is L_1^h, AND $\cdots$ AND$\varphi_\mathfrak{b}(\mathbf{x}_f(\mathbf{k}))$ is $L_\mathfrak{b}^h$, **THEN**

$$\begin{aligned}\mathbf{x}_f(\mathbf{k}+1) &= A_{fh,\Upsilon(\mathbf{k})}\mathbf{x}_f(\mathbf{k}) + B_{fh,\Upsilon(\mathbf{k})}\bar{\mathbf{y}}(\mathbf{k}) \\ r_f(\mathbf{k}) &= C_{fh,\Upsilon(\mathbf{k})}\mathbf{x}_f(\mathbf{k}) + D_{fh,\Upsilon(\mathbf{k})}\bar{\mathbf{y}}(\mathbf{k})\end{aligned} \tag{19}$$

where $\varphi(\mathbf{x}_f(\mathbf{k})) = [\varphi_1(\mathbf{x}_f(\mathbf{k})), \varphi_2(\mathbf{x}_f(\mathbf{k})), \ldots, \varphi_\mathfrak{b}(\mathbf{x}_f(\mathbf{k}))]$ stands for the premise variable, and L_c^h $(h = 1, 2, \ldots, \hbar; c = 1, 2, \ldots, \mathfrak{b})$ are the fuzzy set. $\mathbf{x}_f(\mathbf{k}) \in \mathbb{R}^{\mathbf{n_x}}$ and $r_f(\mathbf{k}) \in \mathbb{R}^{\mathbf{n}_r}$ are the state of fuzzy FD filter and the residual signal, respectively. $A_{fh,\Upsilon(\mathbf{k})}, B_{fh,\Upsilon(\mathbf{k})}, C_{fh,\Upsilon(\mathbf{k})}$, and $D_{fh,\Upsilon(\mathbf{k})}$ denote the filter gain matrices. The activation intensity of the jth fuzzy rule can be described as $\mathcal{L}_h(\mathbf{x}_f(\mathbf{k})) = [\underline{\iota}_h(\mathbf{x}_f(\mathbf{k})), \bar{\iota}_h(\mathbf{x}_f(\mathbf{k}))]$, where $\underline{\iota}_h(\mathbf{x}_f(\mathbf{k})) = \prod_{\epsilon=1}^{\mathfrak{b}} \underline{\varkappa}_{L_\epsilon^h}(\varphi_\epsilon(\mathbf{x}_f(\mathbf{k}))) \geq 0$ and $\bar{\iota}_h(\mathbf{x}_f(\mathbf{k})) = \prod_{\epsilon=1}^{\mathfrak{b}} \bar{\varkappa}_{L_\epsilon^h}(\varphi_\epsilon(\mathbf{x}_f(\mathbf{k}))) \geq 0$ are LUMFs, which satisfy $\bar{\iota}_h(\mathbf{x}_f(\mathbf{k})) \geq \underline{\iota}_h(\mathbf{x}_f(\mathbf{k}))$. $\underline{\varkappa}_{L_\epsilon^h}(\varphi_\epsilon(\mathbf{x}_f(\mathbf{k})))$ and $\bar{\varkappa}_{L_\epsilon^h}(\varphi_\epsilon(\mathbf{x}_f(\mathbf{k})))$ are LUMGs which content $\bar{\varkappa}_{L_\epsilon^h}(\varphi_\epsilon(\mathbf{x}_f(\mathbf{k}))) \geq \underline{\varkappa}_{L_\epsilon^h}(\varphi_\epsilon(\mathbf{x}_f(\mathbf{k})))$.

The global fuzzy filter is expressed as follows:

$$\begin{aligned}\mathbf{x}_f(\mathbf{k}+1) &= \sum_{h=1}^{\hbar}\tau_h\left(\mathbf{x}_f(\mathbf{k})\right)\left[A_{fh,\Upsilon(\mathbf{k})}\mathbf{x}_f(\mathbf{k}) + B_{fh,\Upsilon(\mathbf{k})}\bar{\mathbf{y}}(\mathbf{k})\right] \\ r_f(\mathbf{k}) &= \sum_{h=1}^{\hbar}\tau_h\left(\mathbf{x}_f(\mathbf{k})\right)\left[C_{fh,\Upsilon(\mathbf{k})}\mathbf{x}_f(\mathbf{k}) + D_{fh,\Upsilon(\mathbf{k})}\bar{\mathbf{y}}(\mathbf{k})\right]\end{aligned} \tag{20}$$

where

$$\tau_h\left(\mathbf{x}_f(\mathbf{k})\right) = \frac{\hat{\tau}_h\left(\mathbf{x}_f(\mathbf{k})\right)}{\sum_{h=1}^{\hbar}\hat{\tau}_h\left(\mathbf{x}_f(\mathbf{k})\right)} \geq 0, \quad \sum_{h=1}^{\hbar}\tau_h\left(\mathbf{x}_f(\mathbf{k})\right) = 1$$
$$\hat{\tau}_h\left(\mathbf{x}_f(\mathbf{k})\right) = \underline{N}_h\left(\mathbf{x}_f(\mathbf{k})\right)\underline{\iota}_h\left(\mathbf{x}_f(\mathbf{k})\right) + \bar{N}_h\left(\mathbf{x}_f(\mathbf{k})\right)\bar{\iota}_h\left(\mathbf{x}_f(\mathbf{k})\right).$$

$\tau_h(\mathbf{x}_f(\mathbf{k}))$ stands for a normalized membership. The NWFs are represented by $\underline{N}_h(\mathbf{x}_f(\mathbf{k})) \in [0, 1]$ and $\bar{N}_h(\mathbf{x}_f(\mathbf{k})) \in [0, 1]$, and $\underline{N}_h(\mathbf{x}_f(\mathbf{k})) + \bar{N}_h(\mathbf{x}_f(\mathbf{k})) = 1$. For ease of description, let $g_t(\mathbf{x}(\mathbf{k})) \stackrel{\Delta}{=} g_t$ and $\tau_h(\mathbf{x}_f(\mathbf{k})) \stackrel{\Delta}{=} \tau_h$.

D. Fault Weighting System

A fault weighting technique can be introduced to enhance FD performance in this section. Here, $\mathbf{f}_w(z) = N(z)\mathbf{f}(z)$, where $N(z)$ is a function known a priori. The state-space realization of $\mathbf{f}_w(z) = N(z)\mathbf{f}(z)$ is described as follows:

$$\begin{aligned} \mathbf{x}_w(\mathbf{k}+1) &= A_w\mathbf{x}_w(\mathbf{k}) + B_w\mathbf{f}(\mathbf{k}) \\ \mathbf{f}_w(\mathbf{k}) &= C_w\mathbf{x}_w(\mathbf{k}) + D_w\mathbf{f}(\mathbf{k}) \end{aligned} \tag{21}$$

where $\mathbf{x}_w(\mathbf{k}) \in \mathbb{R}^{\mathbf{n}_{\mathbf{x}_w}}$ stands for the state-space vector. A_w, B_w, C_w, and D_w denote the constant matrices.

E. Augmented FD System

Define $\eta(\mathbf{k}) = [\mathbf{x}^T(\mathbf{k}), \bar{\mathbf{y}}^T(\mathbf{k}-1), \mathbf{x}_f^T(\mathbf{k}), \mathbf{x}_w^T(\mathbf{k})]^T$, and $\mathbf{y}(\ell_\mathfrak{p}) = [\mathbf{y}_1^T(\ell_\mathfrak{p}^1), \mathbf{y}_2^T(\ell_\mathfrak{p}^2), \ldots, \mathbf{y}_{\mathbf{n_y}}^T(\ell_\mathfrak{p}^{\mathbf{n_y}})]^T$. In addition, let $\tilde{r}(\mathbf{k}) = r_f(\mathbf{k}) - \mathcal{F}\mathbf{f}_w(\mathbf{k})$, $\mathfrak{p} = \Upsilon(\mathbf{k})$, $\mathfrak{q} = \Upsilon(\mathbf{k}+1)$, and $\mathbf{d}(\mathbf{k}) = [\mathbf{w}^T(\mathbf{k}), \mathbf{f}^T(\mathbf{k})]^T$.

For $\mathbf{k} \in \mathbf{S}_1$, combining (2), (8), and (20), it yields that

$$\begin{aligned} \eta(\mathbf{k}+1) &= \sum_{t=1}^{\hbar}\sum_{h=1}^{\hbar} g_t\tau_h \left[\bar{A}_{\text{th},\mathfrak{p}}\eta(\mathbf{k}) + \bar{E}_{\text{th},\mathfrak{p}}\mathbf{d}(\mathbf{k}) + \bar{C}_{\text{th},\mathfrak{p}}\mathbf{y}(\ell_\mathfrak{p})\right] \\ \tilde{r}(\mathbf{k}) &= \sum_{t=1}^{\hbar}\sum_{h=1}^{\hbar} g_t\tau_h \left[\bar{A}_{1\text{th},\mathfrak{p}}\eta(\mathbf{k}) + \bar{E}_{1\text{th},\mathfrak{p}}\mathbf{d}(\mathbf{k}) \right. \\ &\qquad \left. + \bar{C}_{1\text{th},\mathfrak{p}}\mathbf{y}(\ell_\mathfrak{p})\right] \end{aligned} \tag{22}$$

where

$$\bar{A}_{\text{th},\mathfrak{p}} = \begin{bmatrix} A_t & 0 & 0 & 0 \\ 0 & 0 & 0 & 0 \\ 0 & 0 & A_{fh,\mathfrak{p}} & 0 \\ 0 & 0 & 0 & A_w \end{bmatrix}, \quad \bar{E}_{\text{th},\mathfrak{p}} = \begin{bmatrix} E_t & E_{ft} \\ 0 & 0 \\ 0 & 0 \\ 0 & B_w \end{bmatrix}$$

$$\bar{C}_{\text{th},\mathfrak{p}} = \begin{bmatrix} 0 \\ I \\ E_{ft} \\ 0 \end{bmatrix}, \quad \bar{A}_{1\text{th},\mathfrak{p}} = \begin{bmatrix} 0 & 0 & C_{fh,\mathfrak{p}} & -\mathcal{F}C_w \end{bmatrix}$$

$$\bar{E}_{1\text{th},\mathfrak{p}} = \begin{bmatrix} 0 & -\mathcal{F}D_w \end{bmatrix}, \quad \bar{C}_{1\text{th},\mathfrak{p}} = D_{fh,\mathfrak{p}}.$$

For $\mathbf{k} \in \mathbf{S}_2$, based upon (2), (14), and (20), it follows that:

$$\begin{aligned} \eta(\mathbf{k}+1) &= \sum_{t=1}^{\hbar}\sum_{h=1}^{\hbar} g_t\tau_h \left[\left(\tilde{A}_{1\text{th},\mathfrak{p}} + \tilde{A}_{2\text{th},\mathfrak{p}}\right)\eta(\mathbf{k}) + \tilde{E}_{\text{th},\mathfrak{p}}\mathbf{d}(\mathbf{k})\right] \\ \tilde{r}(\mathbf{k}) &= \sum_{t=1}^{\hbar}\sum_{h=1}^{\hbar} g_t\tau_h \left[\left(\tilde{A}_{3\text{th},\mathfrak{p}} + \tilde{A}_{4\text{th},\mathfrak{p}}\right)\eta(\mathbf{k}) + \tilde{C}_{1\text{th},\mathfrak{p}}\mathbf{d}(\mathbf{k})\right] \end{aligned} \tag{23}$$

where

$$\tilde{A}_{1\text{th},\mathfrak{p}} = \begin{bmatrix} A_t & 0 & 0 & 0 \\ \rho\Psi_\mathfrak{p}C_t & \tilde{\Psi}_\mathfrak{p} & 0 & 0 \\ \rho B_{fh,\mathfrak{p}}\Psi_\mathfrak{p}C_t & B_{fh,\mathfrak{p}}\tilde{\Psi}_\mathfrak{p} & A_{fh,\mathfrak{p}} & 0 \\ 0 & 0 & 0 & A_w \end{bmatrix}$$

$$\tilde{A}_{2\text{th},\mathfrak{p}} = \begin{bmatrix} 0 & 0 & 0 & 0 \\ -\tilde{\upsilon}\Psi_\mathfrak{p}C_t & 0 & 0 & 0 \\ -\tilde{\upsilon}B_{fh,\mathfrak{p}}C_t & 0 & 0 & 0 \\ 0 & 0 & 0 & 0 \end{bmatrix}$$

$$\tilde{E}_{\text{th},\mathfrak{p}} = \begin{bmatrix} E_t & E_{ft} \\ 0 & 0 \\ 0 & 0 \\ 0 & B_w \end{bmatrix}$$

$$\tilde{A}_{3\text{th},\mathfrak{p}} = \begin{bmatrix} \rho D_{fh,\mathfrak{p}}\Psi_\mathfrak{p}C_t & D_{fh,\mathfrak{p}}\tilde{\Psi}_\mathfrak{p} & C_{fh,\mathfrak{p}} & -\mathcal{F}C_w \end{bmatrix}$$

$$\tilde{A}_{4\text{th},\mathfrak{p}} = \begin{bmatrix} -\tilde{\upsilon}D_{fh,\mathfrak{p}}\Psi_\mathfrak{p}C_t & 0 & 0 & 0 \end{bmatrix}, \rho = 1 - \bar{\theta}$$

$$\tilde{C}_{1\text{th},\mathfrak{p}} = \begin{bmatrix} 0 & -\mathcal{F}D_w \end{bmatrix}, \quad \tilde{\upsilon} = \theta(\mathbf{k}) - \bar{\theta}.$$

For $\mathbf{k} \in \mathbf{S}_3$, on the basis of (2), (16), and (20), one has

$$\begin{aligned} \eta(\mathbf{k}+1) &= \sum_{t=1}^{\hbar}\sum_{h=1}^{\hbar} g_t\tau_h \left[\hat{A}_{1\text{th},\mathfrak{p}}\eta(\mathbf{k}) + \hat{E}_{1\text{th},\mathfrak{p}}\mathbf{d}(\mathbf{k})\right] \\ \tilde{r}(\mathbf{k}) &= \sum_{t=1}^{\hbar}\sum_{h=1}^{\hbar} g_t\tau_h \left[\hat{A}_{3\text{th},\mathfrak{p}}\eta(\mathbf{k}) + \hat{E}_{2\text{th},\mathfrak{p}}\mathbf{d}(\mathbf{k})\right] \end{aligned} \tag{24}$$

where

$$\hat{A}_{1\text{th},\mathfrak{p}} = \begin{bmatrix} A_t & 0 & 0 & 0 \\ 0 & I & 0 & 0 \\ 0 & B_{fh,\mathfrak{p}} & A_{fh,\mathfrak{p}} & 0 \\ 0 & 0 & 0 & A_w \end{bmatrix}$$

$$\hat{E}_{1\text{th},\mathfrak{p}} = \begin{bmatrix} E_t & E_{ft} \\ 0 & 0 \\ 0 & 0 \\ 0 & E_{ft} \end{bmatrix}, \quad \hat{E}_{2\text{th},\mathfrak{p}} = \begin{bmatrix} 0 & -\mathcal{F}D_w \end{bmatrix}$$

$$\hat{A}_{3\text{th},\mathfrak{p}} = \begin{bmatrix} 0 & D_{fh,\mathfrak{p}} & C_{fh,\mathfrak{p}} & -\mathcal{F}C_w \end{bmatrix}.$$

In the following, an FD mechanism is described. Similar to [10], we define the residual evaluation function $H(r_f)$ and the FD threshold H_{th} as follows:

$$H(r_f) = \frac{1}{\mathbf{k}}\sqrt{\sum_{\mathbf{k}=0}^{T} r_f^T(\mathbf{k})r_f(\mathbf{k})} \tag{25}$$

$$H_{\text{th}} = \sup_{0\neq\mathbf{w}\in L_2,\mathbf{f}=0} H(r_f). \tag{26}$$

In terms of (25) and (26), the following FD logic is provided to detect the occurrence of faults:

$$H(r_f) > H_{\text{th}} \Longrightarrow \text{with faults} \Longrightarrow \text{alarm} \tag{27}$$

$$H(r_f) < H_{\text{th}} \Longrightarrow \text{no faults}. \tag{28}$$

III. Main Results

In this section, sufficient criteria for the asymptotic stability with H_∞ performance are presented for the FD system incorporating the DAET-WTOD protocol and DoS attacks. Additionally, based on Theorem 1, the design conditions for the FD filter are provided in Theorem 45 [2].

A. Performance Analysis

Theorem 1: Let the fuzzy FD filter gain matrices $A_{fh,\mathfrak{p}}, B_{fh,\mathfrak{p}}$, $C_{fh,\mathfrak{p}}$, and $D_{fh,\mathfrak{p}}$, and positive constants ϕ_ι, λ_ι, $\bar{\sigma}_{\max}$, $\bar{\sigma}_{\min}$, Λ, F, $\bar{F}$, $\bar{\theta}$, $\mathfrak{b}$, μ, $\mho$, ϑ, and γ be given. Assume that the MFs satisfy $\tau_h - \varsigma_h g_h \geq 0$ $(0 < \varsigma_h \leq 1)$ and there exist matrices $G_\mathfrak{p} > 0, M, N, Q$ satisfying $(1 \leq t,\ h \leq \hbar)$

$$\Pi_{\text{th}\mathfrak{pq}} + \Pi_{ht\mathfrak{pq}} - 2M < 0 \tag{29}$$

$$\varsigma_h\Pi_{\text{th}\mathfrak{pq}} + \varsigma_t\Pi_{ht\mathfrak{pq}} - \varsigma_h M - \varsigma_t M + 2M < 0 \tag{30}$$

$$\Theta_{\text{th}\mathfrak{pq}} + \Theta_{ht\mathfrak{pq}} - 2N < 0 \tag{31}$$

$$\varsigma_h\Theta_{\text{th}\mathfrak{pq}} + \varsigma_t\Theta_{ht\mathfrak{pq}} - \varsigma_h N - \varsigma_t N + 2N < 0 \tag{32}$$

This article has been accepted for publication in a future issue of this journal, but has not been fully edited. Content may change prior to final publication. Citation information: DOI 10.1109/TNNLS.2025.3579254, IEEE TRANSACTIONS ON NEURAL NETWORKS AND LEARNING SYSTEMS

$$\Omega_{\mathrm{thpq}} + \Omega_{htpq} - 2Q < 0 \tag{33}$$

$$\varsigma_h \Omega_{\mathrm{thpq}} + \varsigma_t \Omega_{htpq} - \varsigma_h Q - \varsigma_t Q + 2Q < 0 \tag{34}$$

where

$$\Pi_{\mathrm{thpq}} = \begin{bmatrix} F_{1\mathrm{thpq}} & * & * & * \\ F_{2\mathrm{thpq}} & F_{3\mathrm{thpq}} & * & * \\ 0 & 0 & -\bar{F} & * \\ F_{4\mathrm{thpq}} & F_{5\mathrm{thpq}} & 0 & F_{6\mathrm{thpq}} \end{bmatrix}$$

$$F_{1\mathrm{thpq}} = \bar{A}_{\mathrm{thp}}^T G_{\mathrm{q}} \bar{A}_{\mathrm{thp}} - G_{\mathrm{p}} + \bar{A}_{1\mathrm{thp}}^T \bar{A}_{1\mathrm{thp}} + \bar{C}_t^T \mho \bar{C}_t$$

$$F_{2\mathrm{thpq}} = \bar{C}_{\mathrm{thp}}^T G_{\mathrm{q}} \bar{A}_{\mathrm{thp}} + \bar{C}_{1\mathrm{thp}}^T \bar{A}_{1\mathrm{thp}}$$

$$F_{3\mathrm{thpq}} = \bar{C}_{\mathrm{thp}}^T G_{\mathrm{q}} \bar{C}_{\mathrm{thp}} + \bar{C}_{1\mathrm{thp}}^T \bar{C}_{1\mathrm{thp}}$$

$$F_{4\mathrm{thpq}} = \bar{E}_{\mathrm{thp}}^T G_{\mathrm{q}} \bar{A}_{\mathrm{thp}} + \bar{E}_{1\mathrm{thp}}^T \bar{A}_{1\mathrm{thp}}$$

$$F_{5\mathrm{thpq}} = \bar{E}_{\mathrm{thp}}^T G_{\mathrm{q}} \bar{C}_{\mathrm{thp}} + \bar{E}_{1\mathrm{thp}}^T \bar{C}_{1\mathrm{thp}}$$

$$F_{6\mathrm{thpq}} = \bar{E}_{\mathrm{thp}}^T G_{\mathrm{q}} \bar{E}_{\mathrm{thp}} + \bar{E}_{1\mathrm{thp}}^T \bar{E}_{1\mathrm{thp}} - \gamma^2 I$$

$$\Theta_{\mathrm{thpq}} = \begin{bmatrix} \Gamma_{1\mathrm{thpq}} & * \\ \Gamma_{2\mathrm{thpq}} & \Gamma_{3\mathrm{thpq}} \end{bmatrix}$$

$$\Gamma_{1\mathrm{thpq}} = \tilde{A}_{1\mathrm{thp}}^T G_{\mathrm{q}} \tilde{A}_{1\mathrm{thp}} + \breve{A}_{2\mathrm{thp}}^T G_{\mathrm{q}} \breve{A}_{2\mathrm{thp}} + \tilde{A}_{3\mathrm{thp}}^T \tilde{A}_{3\mathrm{thp}} + \breve{A}_{4\mathrm{thp}}^T \breve{A}_{4\mathrm{thp}} - G_{\mathrm{p}}$$

$$\Gamma_{2\mathrm{thpq}} = \tilde{E}_{\mathrm{thp}}^T G_{\mathrm{q}} \tilde{A}_{1\mathrm{thp}} + \tilde{C}_{1\mathrm{thp}}^T \tilde{A}_{3\mathrm{thp}}$$

$$\Gamma_{3\mathrm{thpq}} = \tilde{E}_{\mathrm{thp}}^T G_{\mathrm{q}} \tilde{E}_{\mathrm{thp}} + \tilde{C}_{1\mathrm{thp}}^T \tilde{C}_{1\mathrm{thp}} - \gamma^2 I$$

$$\Omega_{\mathrm{thpq}} = \begin{bmatrix} Y_{1\mathrm{thpq}} & * & * \\ 0 & -\bar{F} & * \\ Y_{2\mathrm{thpq}} & 0 & Y_{3\mathrm{thpq}} \end{bmatrix}$$

$$Y_{1\mathrm{thpq}} = \hat{A}_{1\mathrm{thp}}^T G_{\mathrm{q}} \hat{A}_{1\mathrm{thp}} - G_{\mathrm{p}} + \hat{A}_{3\mathrm{thp}}^T \hat{A}_{3\mathrm{thp}} + \bar{C}_t^T \vartheta \bar{C}_t$$

$$Y_{2\mathrm{thpq}} = \hat{E}_{1\mathrm{thp}}^T G_{\mathrm{q}} \hat{A}_{1\mathrm{thp}} + \hat{E}_{2\mathrm{thp}}^T \hat{A}_{3\mathrm{thp}}$$

$$Y_{3\mathrm{thpq}} = \hat{E}_{1\mathrm{thp}}^T G_{\mathrm{q}} \hat{E}_{1\mathrm{thp}} + \hat{E}_{2\mathrm{thp}}^T \hat{E}_{2\mathrm{thp}} - \gamma^2 I$$

$$\bar{F} = \mu F, \quad \mho = \mu \bar{\sigma}_{\max} \Lambda, \ \bar{C}_t = C_t \breve{E}, \ \vartheta = \mu \bar{\sigma}_{\min} \Lambda$$

$$\breve{E} = \begin{bmatrix} I & 0 & 0 & 0 \end{bmatrix}, \quad \mathfrak{b} = \sqrt{\bar{\theta}\left(1 - \bar{\theta}\right)}$$

$$\breve{A}_{2\mathrm{thp}} = \begin{bmatrix} 0 & 0 & 0 & 0 \\ -\mathfrak{b}\Psi C_t & 0 & 0 & 0 \\ -\mathfrak{b} B_{fh,\mathrm{p}} \Psi C_t & 0 & 0 & 0 \\ 0 & 0 & 0 & 0 \end{bmatrix}$$

$$\breve{A}_{4\mathrm{thp}} = \begin{bmatrix} -\mathfrak{b} D_{fh,\mathrm{p}} \Psi C_t & 0 & 0 & 0 \end{bmatrix}.$$

Then, the FD system is asymptotically stable with H_∞ performance.

Proof: Select the following Lyapunov function:

$$\mathcal{V}(\mathbf{k}) = \eta^T(\mathbf{k}) G_{\mathrm{p}} \eta(\mathbf{k}). \tag{35}$$

In addition, a new variable $\mathcal{J}_D(\mathbf{k})$ can be defined by

$$\mathcal{J}_D(\mathbf{k}) = \Delta\mathcal{V}(\mathbf{k}) + \tilde{r}^T(\mathbf{k})\tilde{r}(\mathbf{k}) - \gamma^2 \mathbf{d}^T(\mathbf{k})\mathbf{d}(\mathbf{k}). \tag{36}$$

Case A: Define

$$\xi_1(\mathbf{k}) = \begin{bmatrix} \eta^T(\mathbf{k}) & \mathbf{y}^T(l_{\mathrm{p}}) & e^T(\mathbf{k}) & \mathbf{d}^T(\mathbf{k}) \end{bmatrix}^T.$$

In accordance with (37) and (38), the difference of $\mathcal{V}(\mathbf{k})$ can be obtained as follows:

$$\begin{aligned} &E\left\{\mathcal{J}_D(\mathbf{k}) \,|\, \mathbf{k} \in \mathbf{S}_1\right\} \\ &\quad \le E\left\{\eta^T(\mathbf{k}+1) G_{\mathrm{q}} \eta(\mathbf{k}+1) - \eta^T(\mathbf{k}) G_{\mathrm{p}} \eta(\mathbf{k}) \right. \\ &\qquad + \tilde{r}^T(\mathbf{k}) \tilde{r}(\mathbf{k}) - \gamma^2 \mathbf{d}^T(\mathbf{k}) \mathbf{d}(\mathbf{k}) \\ &\qquad \left. + \mu\left[\bar{\sigma}_{\max} \mathbf{y}^T(\mathbf{k}) \Lambda \mathbf{y}(\mathbf{k}) - e^T(\mathbf{k}) F e(\mathbf{k})\right]\right\} \\ &\quad = \sum_{t=1}^{\hbar}\sum_{h=1}^{\hbar} g_t \tau_h \xi_1^T(\mathbf{k}) \Pi_{\mathrm{thpq}} \xi_1(\mathbf{k}). \end{aligned} \tag{37}$$

To obtain more relaxed conditions, a slack matrix is introduced as follows:

$$\sum_{t=1}^{\hbar}\sum_{h=1}^{\hbar} g_t (g_h - \tau_h) M = 0. \tag{38}$$

Inserting (38) into (37) yields

$$\begin{aligned} &E\left\{\mathcal{J}_D(\mathbf{k}) \,|\, \mathbf{k} \in \mathbf{S}_1\right\} \\ &\le \sum_{t=1}^{\hbar}\sum_{h=1}^{\hbar} g_t \tau_h \xi_1^T(\mathbf{k}) \Pi_{\mathrm{thpq}} \xi_1(\mathbf{k}) = \frac{1}{2}\sum_{t=1}^{\hbar}\sum_{h=1}^{\hbar} g_t \xi_1^T(\mathbf{k}) \\ &\quad \times \left[g_h\left(\varsigma_h \Pi_{\mathrm{thpq}} + \varsigma_t \Pi_{htpq} - \varsigma_h M - \varsigma_t M + 2M\right)\right. \\ &\qquad \left. + (\tau_h - \varsigma_h g_h)\left(\Pi_{\mathrm{thpq}} + \Pi_{htpq} - 2M\right)\right] \xi_1(\mathbf{k}). \end{aligned} \tag{39}$$

Case B: Based upon (23), defining

$$\xi_2(\mathbf{k}) = \begin{bmatrix} \eta^T(\mathbf{k}) & \mathbf{d}^T(\mathbf{k}) \end{bmatrix}^T$$

one derives

$$\begin{aligned} &E\left\{\mathcal{J}_D(\mathbf{k}) \,|\, \mathbf{k} \in \mathbf{S}_2\right\} \\ &\quad \le E\left\{\eta^T(\mathbf{k}+1) G_{\mathrm{q}} \eta(\mathbf{k}+1) - \eta^T(\mathbf{k}) G_{\mathrm{p}} \eta(\mathbf{k}) \right. \\ &\qquad \left. + \tilde{r}^T(\mathbf{k}) \tilde{r}(\mathbf{k}) - \gamma^2 \mathbf{d}^T(\mathbf{k}) \mathbf{d}(\mathbf{k})\right\} \\ &\quad = \sum_{t=1}^{\hbar}\sum_{h=1}^{\hbar} g_t \tau_h \xi_2^T(\mathbf{k}) \Theta_{\mathrm{thpq}} \xi_2(\mathbf{k}). \end{aligned} \tag{40}$$

By utilizing the same method as in *Case A*, the equation with the slack matrix N is introduced for the inequality (40). Then, one has

$$\begin{aligned} &E\left\{\mathcal{J}_D(\mathbf{k}) \,|\, \mathbf{k} \in \mathbf{S}_2\right\} \\ &\le \frac{1}{2}\sum_{t=1}^{\hbar}\sum_{h=1}^{\hbar} g_t \xi_2^T(\mathbf{k}) \left[g_h\left(\varsigma_h \Theta_{\mathrm{thpq}} + \varsigma_t \Theta_{htpq} - \varsigma_h N - \varsigma_t N\right.\right. \\ &\quad \left.\left. + 2N\right) + (\tau_h - \varsigma_h g_h)\left(\Theta_{\mathrm{thpq}} + \Theta_{htpq} - 2N\right)\right] \xi_2(\mathbf{k}). \end{aligned} \tag{41}$$

Case C: On the basis of (24), defining

$$\xi_3(\mathbf{k}) = \begin{bmatrix} \eta^T(\mathbf{k}) & e^T(\mathbf{k}) & \mathbf{d}^T(\mathbf{k}) \end{bmatrix}^T$$

we obtain

$$\begin{aligned} &E\left\{\mathcal{J}_D(\mathbf{k}) \,|\, \mathbf{k} \in \mathbf{S}_3\right\} \\ &\quad \le E\left\{\eta^T(\mathbf{k}+1) G_{\mathrm{q}} \eta(\mathbf{k}+1) - \eta^T(\mathbf{k}) G_{\mathrm{p}} \eta(\mathbf{k}) \right. \\ &\qquad + \tilde{r}^T(\mathbf{k}) \tilde{r}(\mathbf{k}) - \gamma^2 \mathbf{d}^T(\mathbf{k}) \mathbf{d}(\mathbf{k}) \\ &\qquad \left. + \mu\left[\bar{L}_{\min} \mathbf{y}^T(\mathbf{k}) \Lambda \mathbf{y}(\mathbf{k}) - e^T(\mathbf{k}) F e(\mathbf{k})\right]\right\} \\ &\quad = \sum_{t=1}^{\hbar}\sum_{h=1}^{\hbar} g_t \tau_h \xi_1^T(\mathbf{k}) \Omega_{\mathrm{thpq}} \xi_1(\mathbf{k}). \end{aligned} \tag{42}$$

Similarly, the slack matrix Q is introduced. Then, one has

$$\begin{aligned} &E\left\{\mathcal{J}_D(\mathbf{k}) \,|\, \mathbf{k} \in \mathbf{S}_3\right\} \\ &\le \frac{1}{2}\sum_{t=1}^{\hbar}\sum_{h=1}^{\hbar} g_t \xi_3^T(\mathbf{k}) \end{aligned}$$

$$\times \left[g_h\left(\varsigma_h\Omega_{\text{th}\mathfrak{pq}} + \varsigma_t\Omega_{ht\mathfrak{pq}} - \varsigma_h Q - \varsigma_t Q + 2Q\right) + \left(\tau_h - \varsigma_h g_h\right)\left(\Omega_{\text{th}\mathfrak{pq}} + \Omega_{ht\mathfrak{pq}} - 2Q\right)\right]\xi_3(\mathbf{k}). \quad (43)$$

For the above three cases, under $\tau_h - \varsigma_h g_h \geq 0$, based on (29)–(34), we can obtain

$$E\left\{\mathcal{J}_D(\mathbf{k})\right\} \leq 0. \quad (44)$$

In the case of $\mathbf{d}(\mathbf{k}) = 0$, by using the Schur complement, it can be inferred that $E\{\mathcal{J}_D(\mathbf{k})\} \leq 0$, which implies that the FD system achieves asymptotic stability. Summing both sides of (46), we have $E\{\|\tilde{r}(\mathbf{k})\|_2^2\} - \gamma^2\|\mathbf{d}(\mathbf{k})\|_2^2 < 0$, which implies that the H_∞ performance can be achieved as well. The proof is now complete. ■

B. Asynchronous Fuzzy FD Filter Design

The influence of the DAET-WTOD protocol is reflected in the FD filter gain matrices $A_{fh,\mathfrak{p}}, B_{fh,\mathfrak{p}}, C_{fh,\mathfrak{p}}$, and $D_{fh,\mathfrak{p}}$. In *Case B*, by the means of the DAET-WTOD protocol, we can conclude that $\mathfrak{p} \in \{1, 2, \ldots, \mathbf{n_y}\}$. In addition, since there is no data released, $\mathfrak{p} = 0$ is defined for *Case C*. Besides, $\mathfrak{p} = \mathbf{n_y} + 1$ is defined for *Case A*. Based on the above analysis, it is known that $\mathfrak{p} \in \{0, 1, \ldots, \mathbf{n_y}+1\}$. In the following, Theorem 2 provides the conditions of the fuzzy FD filter design under the proposed DAET-WTOD protocol.

Theorem 2: Let the positive constants $\phi_\iota, \lambda_\iota$, $\bar{\sigma}_{\max}$, $\bar{\sigma}_{\min}$, $\Lambda, F, \bar{F}, \bar{\theta}, \mathfrak{b}, \mu, \mho$, ϑ, and γ be given. Assume that $\tau_h - \varsigma_h g_h \geq 0$ $(0 < \varsigma_h \leq 1)$ is satisfied, and there exist matrices $G_\mathfrak{p} > 0, H_\mathfrak{p} > 0, V_\mathfrak{p} > 0, W_\mathfrak{p} > 0$, and M, N, Q satisfying $(1 \leq t,\ h \leq \hbar)$

$$\begin{bmatrix} 2\vec{G}^1_{\mathfrak{pq}} & * \\ \vec{\Delta}_{\text{th},\mathfrak{p}} + \vec{\Delta}_{ht,\mathfrak{p}} & 2\mathbb{M} \end{bmatrix} < 0 \quad (45)$$

$$\begin{bmatrix} 2\vec{G}^1_{\mathfrak{pq}} & * \\ \sqrt{\varsigma_h}\vec{\Delta}_{\text{th},\mathfrak{p}} + \sqrt{\varsigma_t}\vec{\Delta}_{ht,\mathfrak{p}} & \sqrt{\varsigma_h}\mathbb{M} + \sqrt{\varsigma_t}\mathbb{M} \end{bmatrix} < 0 \quad (46)$$

$$\begin{bmatrix} 2\vec{G}^2_{\mathfrak{pq}} & * \\ \vec{\Sigma}_{\text{th},\mathfrak{p}} + \vec{\Sigma}_{ht,\mathfrak{p}} & 2\mathbb{N} \end{bmatrix} < 0 \quad (47)$$

$$\begin{bmatrix} 2\vec{G}^2_{\mathfrak{pq}} & * \\ \sqrt{\varsigma_h}\vec{\Sigma}_{\text{th},\mathfrak{p}} + \sqrt{\varsigma_t}\vec{\Sigma}_{ht,\mathfrak{p}} & \sqrt{\varsigma_h}\mathbb{N} + \sqrt{\varsigma_t}\mathbb{N} \end{bmatrix} < 0 \quad (48)$$

$$\begin{bmatrix} 2\vec{G}^3_{\mathfrak{pq}} & * \\ \vec{\Xi}_{\text{th},\mathfrak{p}} + \vec{\Xi}_{ht,\mathfrak{p}} & 2\mathbb{Q} \end{bmatrix} < 0 \quad (49)$$

$$\begin{bmatrix} 2\vec{G}^3_{\mathfrak{pq}} & * \\ \sqrt{\varsigma_h}\vec{\Xi}_{\text{th},\mathfrak{p}} + \sqrt{\varsigma_t}\vec{\Xi}_{ht,\mathfrak{p}} & \sqrt{\varsigma_h}\mathbb{Q} + \sqrt{\varsigma_t}\mathbb{Q} \end{bmatrix} < 0 \quad (50)$$

where

$$\begin{aligned}
&A_{fh,\mathfrak{p}} = \hat{H}_\mathfrak{p}^{-1}\bar{A}_{fh,\mathfrak{p}}, \quad B_{fh,\mathfrak{p}} = \hat{H}_\mathfrak{p}^{-1}\bar{B}_{fh,\mathfrak{p}}, \quad \left(\mathfrak{p} = \mathbf{n_y} + 1\right)\\
&A_{fh,\mathfrak{p}} = \hat{V}_\mathfrak{p}^{-1}\tilde{A}_{fh,\mathfrak{p}}\\
&B_{fh,\mathfrak{p}} = \hat{V}_\mathfrak{p}^{-1}\tilde{B}_{fh,\mathfrak{p}}, \quad \left(\mathfrak{p} \in \left\{1, 2, \ldots, \mathbf{n_y}\right\}\right)\\
&A_{fh,\mathfrak{p}} = \hat{W}_\mathfrak{p}^{-1}\vec{A}_{fh,\mathfrak{p}}, \quad B_{fh,\mathfrak{p}} = \hat{W}_\mathfrak{p}^{-1}\vec{B}_{fh,\mathfrak{p}}, \quad (\mathfrak{p} = 0)\\
&C_{fh,\mathfrak{p}} = C_{fh,\mathfrak{p}}, \quad D_{fh,\mathfrak{p}} = D_{fh,\mathfrak{p}}
\end{aligned}$$

and in which

$$\begin{aligned}
\vec{G}^1_{\mathfrak{pq}} &= \text{diag}\left\{G_\mathfrak{q} - He\left\{H_\mathfrak{p}\right\}, G_n - He\left\{H_\mathfrak{p}\right\}, -I, -\mho\right\}\\
\vec{G}^2_{\mathfrak{pq}} &= \text{diag}\left\{G_\mathfrak{q} - He\left\{V_\mathfrak{p}\right\}, G_\mathfrak{q} - He\left\{V_\mathfrak{p}\right\}, -I, -I\right\}\\
\vec{G}^3_{\mathfrak{pq}} &= \text{diag}\left\{G_\mathfrak{q} - He\left\{W_\mathfrak{p}\right\}, G_\mathfrak{q} - He\left\{W_\mathfrak{p}\right\}, -I, -\vartheta\right\}\\
H_\mathfrak{p} &= \text{diag}\left\{\bar{H}_\mathfrak{p}, \bar{H}_\mathfrak{p}, -I, -\theta\right\}\\
\bar{H}_\mathfrak{p} &= \text{diag}\left\{\hat{H}_\mathfrak{p}, \hat{H}_\mathfrak{p}, \hat{H}_\mathfrak{p}, \check{H}_\mathfrak{p}\right\}\\
G_\mathfrak{q} &= \begin{bmatrix} G_{11,\mathfrak{q}} & * & * \\ G_{21,\mathfrak{q}} & G_{22,\mathfrak{q}} & * \\ G_{31,\mathfrak{q}} & G_{32,\mathfrak{q}} & G_{33,\mathfrak{q}} \end{bmatrix}\\
\vec{\Delta}_{\text{th},\mathfrak{p}} &= \begin{bmatrix} \bar{A}^T_{\Delta\text{th},\mathfrak{p}} & 0 & \bar{A}^T_{1\text{th},\mathfrak{p}} & \bar{C}^T_t \\ \bar{C}^T_{\Delta\text{th},\mathfrak{p}} & 0 & \bar{C}^T_{1\text{th},\mathfrak{p}} & 0 \\ 0 & 0 & 0 & 0 \\ \bar{E}^T_{\Delta\text{th},\mathfrak{p}} & 0 & \bar{E}^T_{1\text{th},\mathfrak{p}} & 0 \end{bmatrix}\\
\bar{A}^T_{\Delta\text{th},\mathfrak{p}} &= \begin{bmatrix} A_t^T\hat{H}_\mathfrak{p}^T & 0 & 0 & 0 \\ 0 & 0 & 0 & 0 \\ 0 & 0 & \bar{A}^T_{fh,\mathfrak{p}} & 0 \\ 0 & 0 & 0 & A_w^T\check{H}_\mathfrak{p}^T \end{bmatrix}\\
\bar{E}^T_{\Delta\text{th},\mathfrak{p}} &= \begin{bmatrix} E_t^T\hat{H}_\mathfrak{p}^T & 0 & 0 & 0 \\ E_{ft}^T\hat{H}_\mathfrak{p}^T & 0 & 0 & B_w^T\check{H}_\mathfrak{p}^T \end{bmatrix}\\
\bar{C}^T_{\Delta\text{th},\mathfrak{p}} &= \begin{bmatrix} 0 & \hat{H}_\mathfrak{p}^T & \bar{B}^T_{fh,\mathfrak{p}} & 0 \end{bmatrix}\\
\vec{\Sigma}_{\text{th},\mathfrak{p}} &= \begin{bmatrix} \bar{A}^T_{\Sigma\text{th},\mathfrak{p}} & \check{A}^T_{\Sigma\text{th},\mathfrak{p}} & \tilde{A}^T_{3\text{th},\mathfrak{p}} & \check{A}^T_{4\text{th},\mathfrak{p}} \\ \bar{E}^T_{\Sigma\text{th},\mathfrak{p}} & 0 & \bar{C}^T_{1\text{th},\mathfrak{p}} & 0 \end{bmatrix}\\
V_\mathfrak{p} &= \text{diag}\left\{\bar{V}_\mathfrak{p}, \bar{V}_\mathfrak{p}, I, I\right\}, \quad \bar{V}_\mathfrak{p} = \text{diag}\left\{\hat{V}_\mathfrak{p}, \hat{V}_\mathfrak{p}, \hat{V}_\mathfrak{p}, \check{V}_\mathfrak{p}\right\}\\
\bar{A}^T_{\Sigma\text{th},\mathfrak{p}} &= \begin{bmatrix} A_t^T\hat{V}_\mathfrak{p}^T & \rho C_t^T\Psi_\mathfrak{p}^T\hat{V}_\mathfrak{p}^T & \rho C_t^T\Psi_\mathfrak{p}^T\tilde{B}^T_{fh,\mathfrak{p}} & 0 \\ 0 & \tilde{\Psi}_\mathfrak{p}^T\hat{V}_\mathfrak{p}^T & \tilde{\Psi}_\mathfrak{p}^T\tilde{B}^T_{fh,\mathfrak{p}} & 0 \\ 0 & 0 & \tilde{A}^T_{fh,\mathfrak{p}} & 0 \\ 0 & 0 & 0 & A_w^T\check{V}_\mathfrak{p}^T \end{bmatrix}\\
\bar{E}^T_{\Sigma\text{th},\mathfrak{p}} &= \begin{bmatrix} E_t^T\hat{V}_\mathfrak{p}^T & 0 & 0 & 0 \\ E_{ft}^T\hat{V}_\mathfrak{p}^T & 0 & 0 & E_{ft}^T\check{V}_\mathfrak{p}^T \end{bmatrix}\\
\check{A}^T_{\Sigma\text{th},\mathfrak{p}} &= \begin{bmatrix} 0 & -\mathfrak{b}C_t^T\Psi_\mathfrak{p}^T\hat{V}_\mathfrak{p}^T & -\mathfrak{b}C_t^T\Psi_\mathfrak{p}^T\tilde{B}^T_{fh,\mathfrak{p}} & 0 \\ 0 & \tilde{\Psi}_\mathfrak{p}^T\hat{V}_\mathfrak{p}^T & \tilde{\Psi}_\mathfrak{p}^T\tilde{B}^T_{fh,\mathfrak{p}} & 0 \\ 0 & 0 & \tilde{A}^T_{fh,\mathfrak{p}} & 0 \\ 0 & 0 & 0 & A_w^T\check{V}_\mathfrak{p}^T \end{bmatrix}\\
\vec{\Xi}_{\text{th},\mathfrak{p}} &= \begin{bmatrix} \bar{A}^T_{\Xi\text{th},\mathfrak{p}} & 0 & \hat{A}^T_{3\text{th},\mathfrak{p}} & \bar{C}^T_t \\ 0 & 0 & 0 & 0 \\ \bar{E}^T_{\Xi\text{th},\mathfrak{p}} & 0 & \hat{E}^T_{2\text{th},\mathfrak{p}} & 0 \end{bmatrix}\\
\bar{A}^T_{\Xi\text{th},\mathfrak{p}} &= \begin{bmatrix} A_t^T\hat{W}_\mathfrak{p}^T & 0 & 0 & 0 \\ 0 & \hat{W}_\mathfrak{p}^T & \vec{B}^T_{fh,\mathfrak{p}} & 0 \\ 0 & 0 & \vec{A}^T_{fh,\mathfrak{p}} & 0 \\ 0 & 0 & 0 & A_w^T\hat{W}_\mathfrak{p}^T \end{bmatrix}\\
\bar{E}^T_{\Xi\text{th},\mathfrak{p}} &= \begin{bmatrix} E_t^T\hat{W}_\mathfrak{p}^T & 0 & 0 & 0 \\ E_{ft}^T\hat{W}_\mathfrak{p}^T & 0 & 0 & E_{ft}^T\check{Z}_\mathfrak{p}^T \end{bmatrix}\\
W_\mathfrak{p} &= \text{diag}\left\{\bar{W}_\mathfrak{p}, \bar{W}_\mathfrak{p}, I, I\right\}\\
\bar{W}_\mathfrak{p} &= \text{diag}\left\{\hat{W}_\mathfrak{p}, \hat{W}_\mathfrak{p}, \hat{W}_\mathfrak{p}, \check{W}_\mathfrak{p}\right\}
\end{aligned}$$

$$\mathbb{M} = \mathrm{diag}\left\{-G_{\mathfrak{p}}, 0, -\bar{F}, -\gamma^2 I\right\} - M$$
$$\mathbb{N} = \mathrm{diag}\left\{-G_{\mathfrak{p}}, -\gamma^2 I\right\} - N$$
$$\mathbb{Q} = \mathrm{diag}\left\{-G_{\mathfrak{p}}, -\bar{F}, -\gamma^2 I\right\} - Q.$$

Then, the FD system is asymptotically stable with H_∞ performance.

Proof: By utilizing Schur complement to the conditions (29)–(34), the following inequalities can be obtained:

$$\begin{bmatrix} 2\tilde{G}^1_{\mathfrak{q}} & * \\ \Delta_{\mathrm{th},\mathfrak{p}} + \Delta_{ht,\mathfrak{p}} & 2\mathbb{M} \end{bmatrix} < 0 \tag{51}$$

$$\begin{bmatrix} 2\tilde{G}^1_{\mathfrak{q}} & * \\ \sqrt{\varsigma_h}\Delta_{\mathrm{th},\mathfrak{p}} + \sqrt{\varsigma_t}\Delta_{ht,\mathfrak{p}} & \sqrt{\varsigma_h}\mathbb{M} + \sqrt{\varsigma_t}\mathbb{M} \end{bmatrix} < 0 \tag{52}$$

$$\begin{bmatrix} 2\tilde{G}^2_{\mathfrak{q}} & * \\ \Sigma_{\mathrm{th},\mathfrak{p}} + \Sigma_{ht,\mathfrak{p}} & 2\mathbb{N} \end{bmatrix} < 0 \tag{53}$$

$$\begin{bmatrix} 2\tilde{G}^2_{\mathfrak{q}} & * \\ \sqrt{\varsigma_h}\Sigma_{\mathrm{th},\mathfrak{p}} + \sqrt{\varsigma_t}\Sigma_{ht,\mathfrak{p}} & \sqrt{\varsigma_h}\mathbb{N} + \sqrt{\varsigma_t}\mathbb{N} \end{bmatrix} < 0 \tag{54}$$

$$\begin{bmatrix} 2\tilde{G}^3_{\mathfrak{q}} & * \\ \Xi_{\mathrm{th},\mathfrak{p}} + \Xi_{ht,\mathfrak{p}} & 2\mathbb{Q} \end{bmatrix} < 0 \tag{55}$$

$$\begin{bmatrix} 2\tilde{G}^3_{\mathfrak{q}} & * \\ \sqrt{\varsigma_h}\Xi_{\mathrm{th},\mathfrak{p}} + \sqrt{\varsigma_t}\Xi_{ht,\mathfrak{p}} & \sqrt{\varsigma_h}\mathbb{Q} + \sqrt{\varsigma_t}\mathbb{Q} \end{bmatrix} < 0 \tag{56}$$

where

$$\tilde{G}^1_{\mathfrak{q}} = \mathrm{diag}\left\{-G^{-1}_{\mathfrak{q}}, -G^{-1}_{\mathfrak{q}}, -I, -\mho\right\}$$
$$\tilde{G}^2_{\mathfrak{q}} = \mathrm{diag}\left\{-G^{-1}_{\mathfrak{q}}, -G^{-1}_{\mathfrak{q}}, -I, -I\right\}$$
$$\tilde{G}^2_{\mathfrak{q}} = \mathrm{diag}\left\{-G^{-1}_{\mathfrak{q}}, -G^{-1}_{\mathfrak{q}}, -I, -\vartheta\right\}$$
$$\Delta_{\mathrm{th},\mathfrak{p}} = \begin{bmatrix} \bar{A}^T_{\mathrm{th},\mathfrak{p}} & 0 & \bar{A}^T_{1\mathrm{th},\mathfrak{p}} & \bar{C}^T_t \\ \bar{C}^T_{\mathrm{th},\mathfrak{p}} & 0 & \bar{C}^T_{1\mathrm{th},\mathfrak{p}} & 0 \\ 0 & 0 & 0 & 0 \\ \bar{B}^T_{\mathrm{th},\mathfrak{p}} & 0 & \bar{B}^T_{1\mathrm{th},\mathfrak{p}} & 0 \end{bmatrix}$$
$$\Sigma_{\mathrm{th},\mathfrak{p}} = \begin{bmatrix} \tilde{A}^T_{1\mathrm{th},\mathfrak{p}} & \check{A}^T_{2\mathrm{th},\mathfrak{p}} & \tilde{A}^T_{3\mathrm{th},\mathfrak{p}} & \check{A}^T_{4\mathrm{th},\mathfrak{p}} \\ \tilde{B}^T_{\mathrm{th},\mathfrak{p}} & 0 & \tilde{C}^T_{1\mathrm{th},\mathfrak{p}} & 0 \end{bmatrix}$$
$$\Xi_{\mathrm{th},\mathfrak{p}} = \begin{bmatrix} \hat{A}^T_{1\mathrm{th},\mathfrak{p}} & 0 & \hat{A}^T_{3\mathrm{th},\mathfrak{p}} & \bar{C}^T_t \\ 0 & 0 & 0 & 0 \\ \hat{B}^T_{1\mathrm{th},\mathfrak{p}} & 0 & \hat{B}^T_{2\mathrm{th},\mathfrak{p}} & 0 \end{bmatrix}.$$

Pre- and postmultiply (51)–(56) by $\mathrm{diag}\{H_{\mathfrak{p}}, H_{\mathfrak{p}}, I, I, I, I, I, I\}$ and its transpose, $\mathrm{diag}\{V_{\mathfrak{p}}, V_{\mathfrak{p}}, I, I, I, I\}$ and its transpose, and $\mathrm{diag}\{W_{\mathfrak{p}}, W_{\mathfrak{p}}, I, I, I, I, I\}$ and its transpose, respectively. For $\mathfrak{p} = \mathbf{n_y} + 1$, let $\bar{A}^T_{fh,\mathfrak{p}} = A_{fh,\mathfrak{p}}\hat{H}^T_{\mathfrak{p}}$ and $\bar{B}^T_{fh,\mathfrak{p}} = B_{fh,\mathfrak{p}}\hat{H}^T_{\mathfrak{p}}$. For $\mathfrak{p} \in \{1, 2, \ldots, \mathbf{n_y}\}$, let $\tilde{A}^T_{fh,\mathfrak{p}} = A_{fh,\mathfrak{p}}\hat{V}^T_{\mathfrak{p}}$ and $\tilde{B}^T_{fh,\mathfrak{p}} = B_{fh,\mathfrak{p}}\hat{V}^T_{\mathfrak{p}}$. For $\mathfrak{p} = 0$, let $\vec{A}^T_{fh,\mathfrak{p}} = A_{fh,\mathfrak{p}}\hat{W}^T_{\mathfrak{p}}$ and $\vec{B}^T_{fh,\mathfrak{p}} = B_{fh,\mathfrak{p}}\hat{W}^T_{\mathfrak{p}}$. Then, one derives

$$\begin{bmatrix} 2\bar{G}^1_{\mathfrak{p}\mathfrak{q}} & * \\ \vec{\Delta}_{\mathrm{th},\mathfrak{p}} + \vec{\Delta}_{ht,\mathfrak{p}} & 2\mathbb{M} \end{bmatrix} < 0 \tag{57}$$

$$\begin{bmatrix} 2\bar{G}^1_{\mathfrak{p}\mathfrak{q}} & * \\ \sqrt{\varsigma_h}\vec{\Delta}_{\mathrm{th},\mathfrak{p}} + \sqrt{\varsigma_t}\vec{\Delta}_{ht,\mathfrak{p}} & \sqrt{\varsigma_h}\mathbb{M} + \sqrt{\varsigma_t}\mathbb{M} \end{bmatrix} < 0 \tag{58}$$

$$\begin{bmatrix} 2\bar{G}^2_{\mathfrak{p}\mathfrak{q}} & * \\ \vec{\Sigma}_{\mathrm{th},\mathfrak{p}} + \vec{\Sigma}_{ht,\mathfrak{p}} & 2\mathbb{N} \end{bmatrix} < 0 \tag{59}$$

$$\begin{bmatrix} 2\bar{G}^2_{\mathfrak{p}\mathfrak{q}} & * \\ \sqrt{\varsigma_h}\vec{\Sigma}_{\mathrm{th},\mathfrak{p}} + \sqrt{\varsigma_t}\vec{\Sigma}_{ht,\mathfrak{p}} & \sqrt{\varsigma_h}\mathbb{N} + \sqrt{\varsigma_t}\mathbb{N} \end{bmatrix} < 0 \tag{60}$$

$$\begin{bmatrix} 2\bar{G}^3_{\mathfrak{p}n} & * \\ \vec{\Xi}_{\mathrm{th},\mathfrak{p}} + \vec{\Xi}_{ht,\mathfrak{p}} & 2\mathbb{Q} \end{bmatrix} < 0 \tag{61}$$

$$\begin{bmatrix} 2\bar{G}^3_{\mathfrak{p}\mathfrak{q}} & * \\ \sqrt{\varsigma_h}\vec{\Xi}_{\mathrm{th},\mathfrak{p}} + \sqrt{\varsigma_t}\vec{\Xi}_{ht,\mathfrak{p}} & \sqrt{\varsigma_h}\mathbb{Q} + \sqrt{\varsigma_t}\mathbb{Q} \end{bmatrix} < 0 \tag{62}$$

where

$$\bar{G}^1_{\mathfrak{p}\mathfrak{q}} = \mathrm{diag}\left\{-H_{\mathfrak{p}}G^{-1}_{\mathfrak{q}}H^T_{\mathfrak{p}}, -H_{\mathfrak{p}}G^{-1}_{\mathfrak{q}}H^T_{\mathfrak{p}}, -I, -\mho\right\}$$
$$\bar{G}^2_{\mathfrak{p}\mathfrak{q}} = \mathrm{diag}\left\{-V_{\mathfrak{p}}G^{-1}_{\mathfrak{q}}V^T_{\mathfrak{p}}, -V_{\mathfrak{p}}G^{-1}_{\mathfrak{q}}V^T_{\mathfrak{p}}, -I, -I\right\}$$
$$\bar{G}^3_{\mathfrak{p}\mathfrak{q}} = \mathrm{diag}\left\{-W_{\mathfrak{p}}G^{-1}_{\mathfrak{q}}W^T_{\mathfrak{p}}, -W_{\mathfrak{p}}G^{-1}_{\mathfrak{q}}W^T_{\mathfrak{p}}, -I, -\vartheta\right\}.$$

Moreover, for positive-define matrices $G_{\mathfrak{q}}$, similar to [9], $G_{\mathfrak{q}} - He\{H_{\mathfrak{p}}\}, G_{\mathfrak{q}} - He\{Y_{\mathfrak{p}}\}$, and $G_{\mathfrak{q}} - He\{Z_{\mathfrak{p}}\}$ are utilized to replace $-H_{\mathfrak{p}}G^{-1}_{\mathfrak{q}}H^T_{\mathfrak{p}}, -V_{\mathfrak{p}}G^{-1}_{\mathfrak{q}}V^T_{\mathfrak{p}}$, and $-W_{\mathfrak{p}}G^{-1}_{\mathfrak{q}}W^T_{\mathfrak{p}}$, respectively. Then, the conditions of the fuzzy FD filter design (45)–(50) are obtained, and the proof is completed. ∎

Remark 4: In accordance with the IPM technique, due to the introduction of equations with slack matrices during the system performance analysis process in Theorem 1, the fuzzy FD filter MFs are freely chosen within the allowed range specified in the following:

$$\begin{cases} \varsigma_1 g_1 \leq \tau_1 \leq 1 \\ \varsigma_2 g_2 \leq \tau_2 \leq 1 \\ \quad\vdots \\ \varsigma_{\hbar-1} g_{\hbar-1} \leq \tau_{\hbar-1} \leq 1 \\ \varsigma_\hbar g_\hbar \leq \tau_\hbar \leq 1. \end{cases} \tag{63}$$

It should be particularly noted that, within the IPM technique, the fuzzy filter MFs [25], [26] are generally constructed based on the designers' work experience and subjective intuition. While this traditional method of selecting filter MFs can ensure the stability of the fuzzy systems, it cannot achieve optimal H_∞ performance.

Remark 5: It is obvious that different system performance outcomes can be achieved depending on the design of the MFs. Consequently, we are committed to exploring an MF optimization technique aimed at enhancing H_∞ performance. To achieve this, the opposition-based learning algorithm is proposed for the first time. Define

$$\mathbb{T} = [\tau_1, \tau_2, \ldots, \tau_\hbar]^T \in \mathbb{R}^\hbar$$

as the population, where τ_ι $(\iota = 1, 2, \ldots, \hbar)$ is considered as an individual. The main objective in this article is to find the optimal values $\mathbb{T}^* = [\tau^*_1, \tau^*_2, \ldots, \tau^*_\hbar]^T$ that satisfy the following fitness function:

$$f(\tau_1, \tau_2, \ldots, \tau_\hbar) = \min_{\mathbb{T}\in\Omega} \|\tilde{r}(\mathbf{k})\| \tag{64}$$

where $\Omega \in \mathbb{R}^\hbar$ represents the feasible value space of $\mathbb{T}$.

C. MF Optimization With Opposition-Based Learning ADE Algorithm

In this section, the new MF online iteration procedure using the opposition-based learning ADE algorithm is presented to achieve improved H_∞ performance, specifically enhancing the disturbance attenuation ability for networked IT2 T-S fuzzy systems. The differential evolution (DE) algorithm, known for its effectiveness in multiobjective optimization, is employed to address optimization problems in multidimensional spaces. The key core steps of the DE algorithm include hybridization, mutation, and replication manipulations. The designed ADE method offers advantages such as ease of implementation, fast convergence, and fewer parameters. The detailed optimization process of the ADE approach is outlined as follows.

1) Set Initial Population: For the provided ADE algorithm, the boundaries of each variable should be determined first at the beginning of the algorithm. Thereupon, the lower and upper bounds (LUBs) of the filter MFs should be determined in advance. Considering the filter MFs limitation $\sum_{s=1}^{\hbar} \tau_s = 1$ that must be guaranteed during the optimization iteration process, $\hbar-1$ filter MFs $\tau_1, \tau_2, \ldots, \tau_{\hbar--1}$ are taken into account, and the filter MF $\tau_\hbar$ is devised based on $\tau_\hbar = 1 - \sum_{\beta=1}^{\hbar--1} \tau_\beta$. Moreover, since the lower bound of $\hbar$th filter MF $\tau_\hbar$ is $\varsigma_\hbar g_\hbar$, consequently, the sum of the $\hbar--1$ filter MFs cannot exceed $1 - \varsigma_\hbar g_\hbar$.

In accordance with the foregoing discussion, the LUBs of each filter MFs τ_l $(l = 1, 2, \ldots, \hbar - 1)$ are further deduced by

$$\begin{cases} \tau_{1\min} = \varsigma_1 \leq \tau_1 \leq \dfrac{1 - \sum_{t=1}^{\hbar} \varsigma_t + \varsigma_1}{\Gamma} = \tau_{1\max} \\ \tau_{2\min} = \varsigma_2 \leq \tau_2 \leq \dfrac{1 - \sum_{t=1}^{\hbar} \varsigma_t + \varsigma_2}{\Gamma} = \tau_{2\max} \\ \qquad\vdots \\ \tau_{\hbar-1\min} = \varsigma_{\hbar-1} \leq \tau_{\hbar-1} \leq \dfrac{1 - \sum_{t=1}^{\hbar} \varsigma_t + \varsigma_{\hbar-1}}{\Gamma} = \tau_{\hbar-1\max} \end{cases} \tag{65}$$

where

$$\Gamma = \frac{\hbar - 1 - (\hbar - 1)\sum_{t=1}^{\hbar} \varsigma_t + \sum_{t=1}^{\hbar-1} \varsigma_t}{1 - \varsigma_\hbar}.$$

Hence, $\Omega = [\tau_{1\min}, \tau_{1\max}] \times \cdots \times [\tau_{\hbar\min}, \tau_{\hbar\max}]$. Then, the size of population **NP** should be determined.

For the ADE algorithm, it is crucial to select an appropriate initial population. If the population size **NP** is too small, the ADE algorithm may converge prematurely or even stagnate. On the other hand, the computational burden may increase, and the convergence speed may significantly slow down if the population size is set too large. After determining the size of the initial population, the operation (66) is performed to obtain the initial individuals

$$\tau_N^0 = \tau_{\min} + \mathrm{diag}\left\{\underbrace{\mathrm{rand}, \ldots, \mathrm{rand}}_{\hbar-1}\right\} \times (\tau_{\max} - \tau_{\min}) \tag{66}$$

where $\tau_{\min} = [\tau_{1\min}, \ldots, \tau_{\hbar-1\min}]^T$ and $\tau_{\max} = [\tau_{1\max}, \ldots, \tau_{\hbar-1\max}]^T$.

A random scalar belonging to $(0, 1)$ is described by the symbol rand. The initial population can be represented by the superscript 0. In addition, the Nth individual is represented by the subscript N.

2) Mutation: To produce the new mutants, the ADE algorithm can stochastically select three different individuals. Subsequently, two of them can be calculated by subtracting and adjusting to produce a new result. In addition, the obtained result can be combined with the remaining individual

$$\begin{gathered} V_N^{\mathbf{k}} = \tau_{N_1}^{\mathbf{k}} + \alpha^{\mathbf{k}}\left(\tau_{N_2}^{\mathbf{k}} - \tau_{N_3}^{\mathbf{k}}\right) \\ N_1, N_2, N_3 \in \{1, \ldots, \mathbf{NP}\}, \text{ and } N \neq N_1 \neq N_2 \neq N_3 \end{gathered} \tag{67}$$

and

$$\alpha^{\mathbf{k}+1} = \begin{cases} \alpha_l + r_1 \times \alpha_u, & \text{if } r_2 < \varepsilon_1 \\ \alpha^{\mathbf{k}}, & \text{otherwise} \end{cases} \tag{68}$$

where the Nth mutant and the Nth individual are represented by $V_N^{\mathbf{k}}$ and $\tau_N^{\mathbf{k}}$, respectively, in $\mathbf{k}$ th generation. An adaptive scale parameter $\alpha^{\mathbf{k}}$ is utilized for controlling the impact of difference item. $r_1 \in [0, 1]$ and $r_2 \in [0, 1]$ denote independent stochastic values. ε_1 stands for the probability of adjusting the adaptive scale parameter $\alpha^{\mathbf{k}}$. α_l and α_u are given parameters that satisfy $0 \leq \alpha_l \leq \alpha_u \leq 1$, in which $\alpha_u = 1 - \alpha_l$. Based on the adaptive rule (68), one can derive $\alpha^{\mathbf{k}} \in [\alpha_l, 1]$.

3) Crossover: For the ADE algorithm, the cross manipulation can enhance the species diversity and make the population as rich as possible. In addition, the cross manipulation can pick excellent individuals and insert them into the current population.

Next, the specific operation rule is given as follows:

$$\theta_{N,\wp}^{\mathbf{k}} = \begin{cases} V_{N,\wp}^{\mathbf{k}}, & \mathrm{rand}(0,1) \leq \mathcal{C}\text{or } \wp = \wp_{\mathrm{rand}} \\ \tau_{N,\wp}^{\mathbf{k}}, & \text{otherwise} \end{cases} \tag{69}$$

in which $\theta_{N,\wp}^{\mathbf{k}}$ stands for the value of the $\wp$ th dimension. The probability of crossover can be represented by $\mathcal{C}$ belonging to $[0, 1]$. For the current population, in the case of $\mathcal{C}$ is small, more information of individuals can be maintained. Instead, it may lead to more individuals changing in the population increasing the number of diversity, and making the search for optimal solutions easier. $\wp_{\mathrm{rand}}$ represents a randomly generated integer. Based on the operation (69), the species diversity can be increased.

4) Selection: The acquired experimental individuals are compared with the target individual. If the fitness is small in the case of using the experimental individual, the target individual may be replaced by the experimental individual. And then, the experimental individual can enter the next generation. In addition, if not, the target individual is used for entering the next generation

$$\tau_N^{\mathbf{k}+1} = \begin{cases} \theta_N^{\mathbf{k}}, & \text{if } f\left(\theta_N^{\mathbf{k}}\right) \leq f\left(\tau_N^{\mathbf{k}}\right) \\ \tau_N^{\mathbf{k}}, & \text{otherwise.} \end{cases} \tag{70}$$

The best values of the filter MFs $\tau_1^*, \ldots, \tau_\hbar^*$ that can minimize the fitness functions (64) are singled out. Then, the global fuzzy FD filter is designed by combining the best filter MFs with the obtained fuzzy filter gains.

Opposition-based learning [27] has been proven to be an effective search approach. It is a commonly utilized optimization strategy in machine learning that identifies the reverse solutions of the current solutions at each iteration of the algorithm. The algorithm then selects the solution that is more favorable for evolution from both the current solution set and the reverse solution set. Leveraging the inherent advantages of opposition-based learning, a new MF online iterative learning algorithm is proposed to find the optimal MF values for the fuzzy FD filter.

Based on the definitions of opposite number and opposite point, an opposition operation is introduced as follows.

1) *Opposition-Based Optimization:* Set $\mathscr{M} = (\varkappa_1, \varkappa_2, \ldots, \varkappa_z)$ to be a point for z-dimensional space, where $\varkappa_\jmath \in [a_\jmath, b_\jmath]$, $\jmath = 1, 2, \ldots, z$. The opposite $\check{\mathscr{M}} = (\check{\varkappa}_1, \check{\varkappa}_2, \ldots, \check{\varkappa}_z)$ can be obtained by the following equation:

$$\check{\varkappa}_\rho = a_\jmath + b_\jmath - \varkappa_\jmath. \tag{71}$$

Based on the fitness function $f(\cdot)$ (64), if $f(\check{\mathscr{M}}) \leq f(\mathscr{M})$, the point $\mathscr{M}$ is replaced by $\check{\mathscr{M}}$; otherwise, the point $\mathscr{M}$ remains unchanged. By evaluating the point and its opposite point, the more suitable point can continue to be utilized.

Combining the ADE algorithm with opposition-based optimization, a new ADE approach is designed to achieve better H_∞ performance for IT2 fuzzy systems. The detailed process of designing the FD filter with optimal H_∞ performance is outlined in s.

Remark 6: In this article, a new FD scheme has been developed for networked IT2 fuzzy systems subjected to stochastic cyberattacks by utilizing a novel DAET-WTOD protocol. Compared to existing results, this article exhibits the following distinctive novelties.

1) *DAET-WTOD Protocol:* A new DAET-WTOD protocol is proposed, which integrates an adaptive ET mechanism with the WTOD protocol. This protocol effectively manages the data transmission of distributed sensors, adjusting the thresholds based on real-time system dynamics and the probability of DoS attacks. This approach conserves communication resources and maintains FD performance under stochastic cyberattacks.
2) *Fuzzy FD Filter Design:* A fuzzy switched-like FD filter with asynchronous MFs is designed to diagnose system faults in networked IT2 fuzzy systems, considering the DAET-WTOD protocol and stochastic cyberattacks.
3) *MF Optimization Using ADE Algorithm:* An opposition-based learning ADE algorithm is introduced to optimize the MFs of the fuzzy FD filter in real time. This optimization technique is shown to enhance the H_∞ performance, achieving better disturbance attenuation by finding the optimal MF values.
4) *Simulation Validation:* Extensive simulations are conducted to demonstrate the effectiveness of the proposed FD method. The results show that the DAET-WTOD protocol further conserves communication resources compared to existing methods, and the opposition-based learning ADE algorithm improves H_∞ performance. Additionally, the proposed FD technique effectively detects system faults even under malicious DoS attacks.

Algorithm 1 FD filter design under MF online learning scheme.

Give the opposition probability $\wp_0$ and the parameters γ, α_l, α_u, r_1, r_2.
In accordance with the conditions (45)–(50) of Theorem 2, the gains of the fuzzy FD filter $A_{fh,\mathfrak{p}}$, $B_{fh,\mathfrak{p}}$, $C_{fh,\mathfrak{p}}$ and $D_{fh,\mathfrak{p}}$ are obtained.
Buffer $A_{fh,\mathfrak{p}}, B_{fh,\mathfrak{p}}, C_{fh,\mathfrak{p}}$ and $D_{fh,\mathfrak{p}}$.
Acquire LUBs of each filter MFs $\tau_{1\min}$-$\tau_{\hbar-1\min}$ and $\tau_{1\max}$-$\tau_{\hbar-1\max}$ in light of the operation (65).
Define the population size **NP**, scaling factors α_l, α_u, r_1, r_2, and crossover probability $\mathcal{C}$. Based on the operation (66), the initial population is obtained.
Let gen = **N** in which the maximum iteration can be represented by **N**.
for $\mathbf{k} = 0 : gen$
Perform the mutation (67) to produce the result $V_N^{\mathbf{k}}$. Based on the crossover operation (69) and the selection operation (70), the group $\mathbb{T}^* = [\tau_1^*, \tau_2^*, \ldots, \tau_\hbar^*]$ is obtained.
/* **Opposition-Based Generation Jumping** */
 if $(rand(0,1) < \wp_0)$
  for $h = 1 : \hbar - 1$
   for $l = 1 : gen$
    $\check{\tau}_{hl}^{*\mathbf{k}} = \tau_{h\min} + \tau_{h\max} - \tau_l^{\mathbf{k}}$
    if $(f(\check{\tau}_{hl}^{*\mathbf{k}}) \leq f(\tau_h^*)$
     $\tau_h^* = \check{\tau}_{hl}^{*\mathbf{k}}$
    else
     $\tau_h^* = \tau_h^*$
    end if
   end for
  end for
end if
 Store the optimal group $\tau_N^{\mathbf{k}*} = \left\{\tau_1^*, \tau_2^*, \ldots, \tau_{\hbar-1}^*, 1 - \sum_{\beta=1}^{\hbar-1} \tau_\beta^*\right\}$.
By combining $\tau_N^{\mathbf{k}*}$ with fuzzy FD gains $A_{fh,\mathfrak{p}}$, $B_{fh,\mathfrak{p}}$, $C_{fh,\mathfrak{p}}$ and $D_{fh,\mathfrak{p}}$, the optimal FD strategy can be devised for the IT2 fuzzy system (2).
 Output the evaluation $\tilde{\mathbf{r}}(\mathbf{k})$.
  if $\mathbf{k} > N$ **then**
   Stop the iteration.
  end if
 end for

Overall, this article has introduced and validated a comprehensive FD scheme that addresses the challenges of data transmission, FD, and system stability in the presence of cyberattacks in networked IT2 fuzzy systems.

IV. Simulation Results

In this section, some simulation results are provided to demonstrate the effectiveness and advantages of the proposed FD method under the new DAET-WTOD protocol and the opposition-based learning ADE policy. The FD scheme is illustrated using the tunnel diode circuit plant. The model is

This article has been accepted for publication in a future issue of this journal, but has not been fully edited. Content may change prior to final publication.
Citation information: DOI 10.1109/TNNLS.2025.3579254, IEEE Transactions on Neural Networks and Learning Systems

described as

$$i_D(\mathbf{k}) = 0.002v_D(\mathbf{k}) + \partial v_D^3(\mathbf{k}) \tag{72}$$

where $\partial \in [0.01, 0.03]$ represents the uncertain parameter. Define $\emptyset = 0.002 + \partial x_1^2(\mathbf{k})$. Then, it can be inferred that

$$\begin{aligned} C\mathbf{x}_1(\mathbf{k}+1) &= -\emptyset\mathbf{x}_1(\mathbf{k}) + \mathbf{x}_2(\mathbf{k}) \\ L\mathbf{x}_2(\mathbf{k}+1) &= -\mathbf{x}_1(\mathbf{k}) - R\mathbf{x}_2(\mathbf{k}) + \mathbf{w}(\mathbf{k}). \end{aligned}$$

Set $C = 20$ mF, $L = 1000$ mH, and $R = 10\ \Omega$. Similar to [10], the IT2 T-S fuzzy model is obtained as follows:

$$\mathbf{x}(\mathbf{k}+1) = \sum_{t=1}^{2} g_t\,[A_t\mathbf{x}(\mathbf{k}) + E_t\mathbf{w}(\mathbf{k})]$$

where

$$A_1 = \begin{bmatrix} \dfrac{-\emptyset_{\min}}{C} & 50 \\ -1 & -10 \end{bmatrix}, \quad E_1 = \begin{bmatrix} 0 \\ 1 \end{bmatrix}$$
$$A_2 = \begin{bmatrix} \dfrac{-\emptyset\max}{C} & 50 \\ -1 & -10 \end{bmatrix}, \quad E_2 = \begin{bmatrix} 0 \\ 1 \end{bmatrix}$$
$$\emptyset_{\min} = 0.001, \quad \emptyset\max = 0.003.$$

Additionally, the remaining system matrices and other matrices used in this article are provided as follows:

$$\begin{aligned} E_{f1} &= \begin{bmatrix} -0.2392 \\ -0.3222 \end{bmatrix}, \quad C_1 = \begin{bmatrix} -0.6808 & -0.1847 \\ 0.0356 & 0.3586 \end{bmatrix} \\ E_{f2} &= \begin{bmatrix} -0.5363 \\ -1.2727 \end{bmatrix}, \quad C_2 = \begin{bmatrix} -0.4113 & -0.0801 \\ 0.1426 & 0.0689 \end{bmatrix} \\ A_w &= -0.9805, \quad B_w = 0.8340, \quad C_w = -0.3526 \\ D_w &= -0.1439. \end{aligned}$$

By using the uncertain parameter $\partial \in [0.01, 0.03]$, the LUMFs of the IT2 T-S fuzzy system are given by

$$\begin{aligned} \underline{\varepsilon}_1(\mathbf{x}_1(\mathbf{k})) &= \frac{\emptyset_{\max} - \emptyset}{\emptyset_{\max} - \emptyset_{\min}}, \quad \text{with } \partial = 0.03 \\ \bar{\varepsilon}_1(\mathbf{x}_1(\mathbf{k})) &= \frac{\emptyset_{\max} - \emptyset}{\emptyset_{\max} - \emptyset_{\min}}, \quad \text{with } \partial = 0.01 \\ \underline{\varepsilon}_2(\mathbf{x}_1(\mathbf{k})) &= \frac{\emptyset - \emptyset_{\min}}{\emptyset_{\max} - \emptyset_{\min}}, \quad \text{with } \partial = 0.01 \\ \bar{\varepsilon}_2(\mathbf{x}_1(\mathbf{k})) &= \frac{\emptyset - \emptyset_{\min}}{\emptyset_{\max} - \emptyset_{\min}}, \quad \text{with } \partial = 0.03. \end{aligned}$$

Based on the IPM technique, the LUMFs of the fuzzy FD filter can be defined by

$$\begin{aligned} &\underline{\iota}_1(\mathbf{x}_{f1}(\mathbf{k})) = 0.3e^{-\mathbf{x}_{f1}^2(\mathbf{k})}, \quad \bar{\iota}_1(\mathbf{x}_{f1}(\mathbf{k})) = \underline{\iota}_1(\mathbf{x}_{f1}(\mathbf{k})) \\ &\underline{\iota}_2(\mathbf{x}_{f1}(\mathbf{k})) = 1 - \bar{\iota}_1(\mathbf{x}_{f1}(\mathbf{k})), \quad \bar{\iota}_2(\mathbf{x}_{f1}(\mathbf{k})) = \underline{\iota}_2(\mathbf{x}_{f1}(\mathbf{k})). \end{aligned}$$

Then, the weighting functions can be provided as follows:

$$\begin{aligned} \underline{H}_t(\mathbf{x}_1(\mathbf{k})) &= \sin^2(\mathbf{x}_1(\mathbf{k})) \\ \bar{H}_t(\mathbf{x}_1(\mathbf{k})) &= 1 - \underline{H}_t(\mathbf{x}_1(\mathbf{k})) \\ \underline{N}_h(\mathbf{x}_{f1}(\mathbf{k})) &= \cos^2(0.6\mathbf{x}_{f1}(\mathbf{k})) \\ \bar{N}_h(\mathbf{x}_{f1}(\mathbf{k})) &= 1 - \underline{N}_h(\mathbf{x}_{f1}(\mathbf{k})). \end{aligned}$$

In this example, two distributed sensor nodes are considered. Consequently, based on the DAET-WTOD protocol, it can be concluded that m belongs to the set $\{0, 1, 2, 3\}$. Set $\mu = 0.65, \underline{\sigma}_{\max} = 1.8, \bar{\sigma}_{\max} = 4.1, \underline{\sigma}_{\min} = 0.8, \bar{\sigma}_{\min} = 0.3, \gamma = 1.45, \varsigma_1 = 0.08, \varsigma_2 = 0.07$, and $\bar{\theta} = 0.2$.

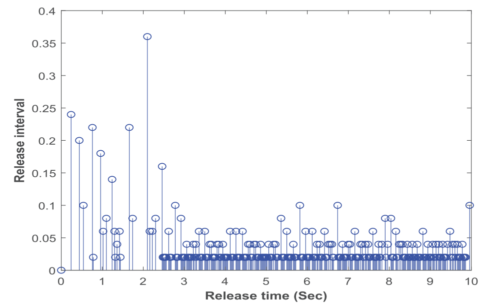

Fig. 2. Release instants of sensor 1 under the DAET-WTOD protocol.

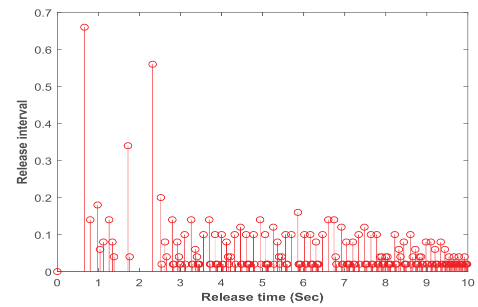

Fig. 3. Release instants of sensor 2 under the DAET-WTOD protocol.

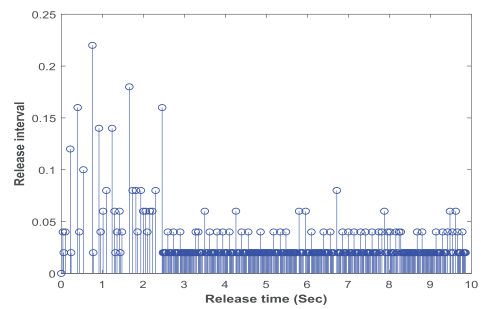

Fig. 4. Release instants of sensor 1 under the existing WTOD protocol [18].

The external disturbance $\mathbf{w}(\mathbf{k})$ and the system fault $\mathbf{f}(\mathbf{k})$ are provided as follows:

$$\mathbf{w}(\mathbf{k}) = \begin{cases} -0.86, & 0 \le \mathbf{k} \le 1.3 \\ 0.72\sin(\mathbf{k}), & 1.3 < \mathbf{k} \le 2.2 \\ 0, & \text{otherwise} \end{cases}$$

and

$$\mathbf{f}(\mathbf{k}) = \begin{cases} 1.12, & 0.9 < \mathbf{k} \le 2.4 \\ 0, & \text{otherwise.} \end{cases}$$

By calculating the linear matrix inequalities (47)–(52), the FD filter gains are obtained. The initial states are set as $\mathbf{x}(0) = [0.04\ \ 0.06]^T$ and $\mathbf{x}_f(0) = [0\ \ 0]^T$. Using the new DAET-WTOD protocol, the signal transmission of the distributed sensors is detailed in Figs. 2 and 3. Fig. 2 shows the signal trigger times for sensor 1, with a total of 309 triggered signals. Fig. 3 illustrates the trigger instants and intervals for sensor 2, with 171 signal transmissions.

For comparison, the signal transmission of the distributed sensors under the existing WTOD data transmission protocol [18] is shown in Figs. 4 and 5. From these figures, it can

This article has been accepted for publication in a future issue of this journal, but has not been fully edited. Content may change prior to final publication. Citation information: DOI 10.1109/TNNLS.2025.3579254,

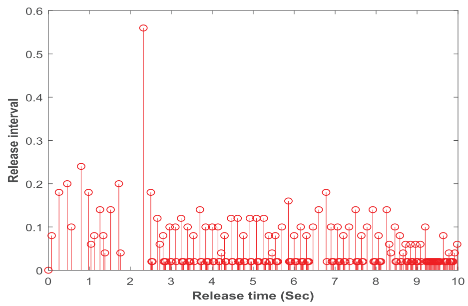

Fig. 5. Release instants of sensor 2 under the existing WTOD protocol [18].

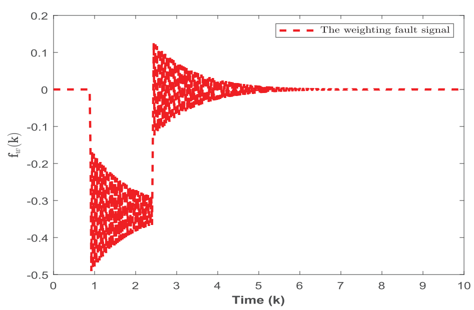

Fig. 6. Weighting fault signal $\mathbf{f}_w(\mathbf{k})$.

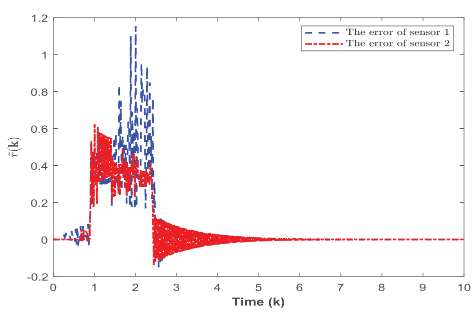

Fig. 7. Error value $\tilde{r}(\mathbf{k})$ of sensors.

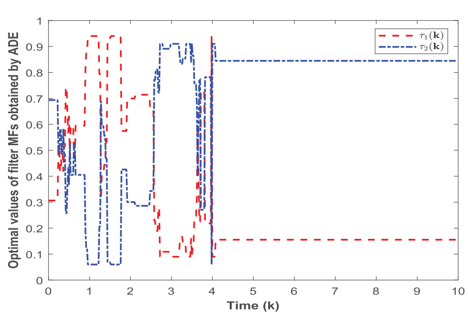

Fig. 8. Fuzzy filter MF trajectories in light of the new MF online learning algorithm.

be observed that sensor 1 released 359 signals, and sensor 2 triggered 197 signals. Comparing Figs. 2–5, it is evident that the proposed DAET-WTOD protocol further conserves limited communication resources. By the means of using the fault weighting technique, the weighting fault signal is depicted in Fig. 6. The error value $\tilde{r}(\mathbf{k})$ between the residual signal and the weighting fault signal is shown in Fig. 7.

Fig. 8 displays the MF iterative trajectories of the fuzzy FD filter using the proposed MF online learning technique with

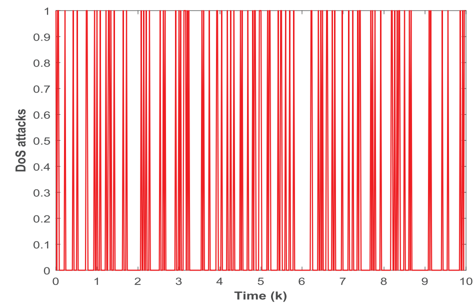

Fig. 9. Distribution of stochastic cyberattacks.

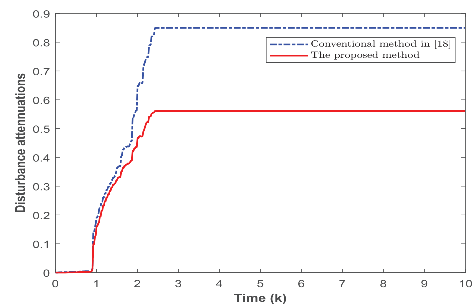

Fig. 10. H_∞ performance levels based on different methods.

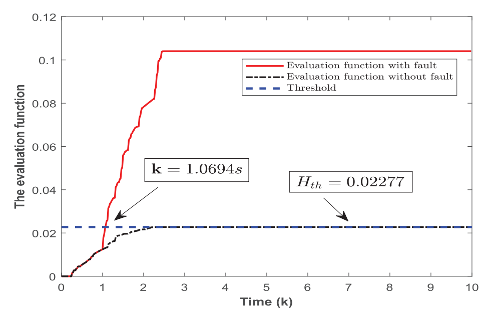

Fig. 11. Evaluation functions under the proposed FD technique.

the opposition-based learning ADE algorithm. Fig. 9 illustrates the occurrence of malicious DoS attacks. Fig. 10 depicts the disturbance attenuation responses under the proposed strategy and the existing method [18]. From Fig. 10, it is clear that the provided MF online optimization technique, using the opposition-based learning ADE algorithm, achieves better H_∞ performance by optimizing the MF values of the fuzzy FD filter.

Fig. 11 demonstrates the effectiveness of FD under the DAET-WTOD protocol and DoS attacks by utilizing the designed FD scheme with the opposition-based learning ADE algorithm. In Fig. 11, the threshold H_{th} is 0.02277, and system faults are detected after 1.0694 s. Summarizing the simulation results, it is determined that the provided FD method conserves network bandwidth more effectively and achieves better H_∞ performance. Additionally, under malicious DoS attacks, the proposed FD technique can effectively detect system fault signals.

V. Conclusion

This article has tackled the challenge of designing an H_∞ optimized FD filter for networked IT2 fuzzy systems subjected to stochastic cyberattacks. A novel DAET-WTOD protocol has been developed to efficiently manage the limited communication bandwidth among distributed sensors. Based on measured output information and attack probability, two adaptive laws have been introduced to dynamically update the triggering thresholds. Furthermore, utilizing the IPM technique, an opposition-based learning ADE algorithm has been proposed which iteratively searches for the optimal MF values of the fuzzy switched-like FD filter to achieve the desired H_∞ performance. Finally, a practical simulation example has been provided to demonstrate the feasibility and advantages of the proposed FD scheme. However, the novel DAET-WTOD protocol and the opposition-based learning ADE algorithm in this proposed scheme may encounter some technical difficulties when executed in complex networked systems and more sophisticated cyberattacks. Therefore, some possible future research topics include, but are not limited to, extension to more complex networked systems [1], [2], [30], robustness against more sophisticated cyberattacks [5], [12], integration with machine learning techniques [21], [45], energy-efficient FD schemes [22], [35], [36], and multiobjective optimization [6], [32], [39].

References

[1] R. Caballero-Águila, A. Hermoso-Carazo and J. Linares-Pérez *Covariance-based fusion filtering for networked systems with random transmission delays, and non-consecutive losses*, "Covariance-based fusion filtering for networked systems with random transmission delays and non-consecutive losses," *Int. J. Gen. Syst.*, vol. 46, no. 7, pp. 752–771, Jun. 2017.

[2] R. Caballero-Águila, A. Hermoso-Carazo, and J. Linares-Pérez, "Networked fusion estimation with multiple uncertainties and time-correlated channel noise," *Inf. Fusion*, vol. 54, pp. 161–171, Feb. 2020.

[3] L. Ding and W. Sun, "Predefined time fuzzy adaptive control of switched fractional-order nonlinear systems with input saturation," *Int. J. Netw. Dyn. Intell.*, vol. 2, no. 4, Dec. 2023, Art. no. 100019.

[4] D. Ding, Z. Wang, and Q.-L. Han, "Neural-network-based output-feedback control with stochastic communication protocols," *Automatica*, vol. 106, pp. 221–229, Aug. 2019.

[5] S.-S. Dong, Y.-G. Li, and L. An, "Optimal strictly stealthy attacks in cyber-physical systems with multiple channels under the energy constraint," *Int. J. Syst. Sci.*, vol. 54, no. 13, pp. 2608–2625, Oct. 2023.

[6] J. Fang, W. Liu, L. Chen, S. Lauria, A. Miron, and X. Liu, "A survey of algorithms, applications and trends for particle swarm optimization," *Int. J. Netw. Dynam. Intell.*, vol. 2, no. 1, pp. 24–50, Mar. 2023.

[7] H. Fang et al., "Fuzzy-based adaptive optimization of unknown discrete-time nonlinear Markov jump systems with off-policy reinforcement learning," *IEEE Trans. Fuzzy Syst.*, vol. 30, no. 12, pp. 5276–5290, Dec. 2022.

[8] Z. Feng, H. Zhang, and H.-K. Lam, "New results on dissipative control for a class of singular Takagi–Sugeno fuzzy systems with time delay," *IEEE Trans. Fuzzy Syst.*, vol. 30, no. 7, pp. 2466–2475, Jul. 2022.

[9] Z. Gu, Y. Fan, X. Sun, X. Xie, and C. K. Ahn, "Event-based two-step transmission mechanism for the stabilization of networked T–S fuzzy systems with random uncertainties," *IEEE Trans. Cybern.*, vol. 54, no. 2, pp. 1283–1293, Feb. 2024.

[10] X. Guo, X. Fan, and C. K. Ahn, "Adaptive event-triggered fault detection for interval type-2 T–S fuzzy systems with sensor saturation," *IEEE Trans. Fuzzy Syst.*, vol. 29, no. 8, pp. 2310–2321, Aug. 2021.

[11] Y. Hu, C. Cai, H. Lin, and O.-M. Kwon, "Fuzzy-model-based H∞ control for networked singularly perturbed systems: The asynchronous weighted try-once-discard protocol case," *IEEE Trans. Fuzzy Syst.*, vol. 32, no. 5, pp. 2713–2724, May 2024.

[12] Y. Jin, X. Ma, X. Meng, and Y. Chen, "Distributed fusion filtering for cyber-physical systems under round-robin protocol: A mixed H_2/H∞ framework," *Int. J. Syst. Sci.*, vol. 54, no. 8, pp. 1661–1675, 2023.

[13] M. Li, J. Liang, and J. Qiu, "Set-membership filtering for 2-D systems under uniform quantization and weighted try-once-discard protocol," *IEEE Trans. Circuits Syst. II, Exp. Briefs*, vol. 70, no. 9, pp. 3474–3478, Sep. 2023.

[14] Q. Li, H. Xue, Y. Pan, and H. Liang, "Dynamic output feedback control for interval type-2 fuzzy systems against DoS attacks and sensor failures," *Int. J. Syst. Sci.*, vol. 54, no. 15, pp. 2904–2920, Apr. 2021.

[15] X. Li, G. Wei, D. Ding, and S. Liu, "Recursive filtering for time-varying discrete sequential systems subject to deception attacks: Weighted try-once-discard protocol," *IEEE Trans. Syst., Man, Cybern., Syst.*, vol. 52, no. 6, pp. 3704–3713, Jun. 2022.

[16] X.-J. Li and G.-H. Yang, "Fault detection in finite frequency domain for Takagi–Sugeno fuzzy systems with sensor faults," *IEEE Trans. Cybern.*, vol. 44, no. 8, pp. 1446–1458, Aug. 2014.

[17] H. Liang, Z. Du, T. Huang, and Y. Pan, "Neuroadaptive performance guaranteed control for multiagent systems with power integrators and unknown measurement sensitivity," *IEEE Trans. Neural Netw. Learn. Syst.*, vol. 34, no. 12, pp. 9771–9782, Dec. 2023.

[18] J. Liu, E. Gong, L. Zha, E. Tian, and X. Xie, "Interval type-2 fuzzy-model-based filtering for nonlinear systems with event-triggering weighted try-once-discard protocol and cyberattacks," *IEEE Trans. Fuzzy Syst.*, vol. 32, no. 3, pp. 721–732, Mar. 2024.

[19] J. L. Liu, E. Y. Gong, L. J. Zha, E. G. Tian, and X. P. Xie, "Observer-based security fuzzy control for nonlinear networked systems under weighted try-once-discard protocol," *IEEE Trans. Fuzzy Syst.*, vol. 31, no. 11, pp. 3853–3865, Nov. 2023.

[20] S. Liu, Z. Wang, L. Wang, and G. Wei, "Finite-horizon H∞ filtering via a high-rate network with the FlexRay protocol," *IEEE Trans. Autom. Control*, vol. 68, no. 6, pp. 3596–3603, Jun. 2023.

[21] X. Luo, Y. Zhong, Z. Wang, and M. Li, "An alternating-direction-method of multipliers-incorporated approach to symmetric non-negative latent factor analysis," *IEEE Trans. Neural Netw. Learn. Syst.*, vol. 34, no. 8, pp. 4826–4840, Aug. 2023.

[22] S. Ma and Y. Li, "Adaptive fuzzy fault-tolerant control for active seat suspension systems with full-state constraints," *Syst. Sci. Control Eng.*, vol. 11, no. 1, Jan. 2023, Art. no. 2153391.

[23] Y. Pan, Q. Li, H. Liang, and H.-K. Lam, "A novel mixed control approach for fuzzy systems via membership functions online learning policy," *IEEE Trans. Fuzzy Syst.*, vol. 30, no. 9, pp. 3812–3822, Sep. 2022.

[24] Y. Pan, Y. Wu, and H. Lam, "Security-based fuzzy control for non-linear networked control systems with DoS attacks via a resilient event-triggered scheme," *IEEE Trans. Fuzzy Syst.*, vol. 30, no. 10, pp. 4359–4368, Oct. 2022.

[25] Y. Pan and G.-H. Yang, "Event-driven fault detection for discrete-time interval type-2 fuzzy systems," *IEEE Trans. Syst., Man, Cybern., Syst.*, vol. 51, no. 8, pp. 4959–4968, Aug. 2021.

[26] W. Qian, Y. Wu, and J. Yang, "Event-driven reduced-order fault detection filter design for nonlinear systems with complex communication channel," *IEEE Trans. Fuzzy Syst.*, vol. 32, no. 1, pp. 281–293, Jul. 2023.

[27] S. Rahnamayan, H. R. Tizhoosh, and M. M. A. Salama, "Opposition-based differential evolution," *IEEE Trans. Evol. Comput.*, vol. 12, no. 1, pp. 64–79, Feb. 2008.

[28] P. Y. Reddy and L. C. Saikia, "Hybrid AC/DC control techniques with improved harmonic conditions using DBN based fuzzy controller and compensator modules," *Syst. Sci. Control Eng.*, vol. 11, no. 1, Dec. 2023, Art. no. 2188406.

[29] M. Shen, T. Zhang, Z.-G. Wu, Q.-G. Wang, and S. Zhu, "Iterative interval estimation-based fault detection for discrete time T–S fuzzy systems," *IEEE Trans. Syst., Man, Cybern., Syst.*, vol. 53, no. 11, pp. 6966–6974, Nov. 2023.

[30] Y. S. Shmaliy, F. Lehmann, S. Zhao, and C. K. Ahn, "Comparing robustness of the Kalman, H∞, and UFIR filters," *IEEE Trans. Signal Process.*, vol. 66, no. 13, pp. 3447–3458, Jul. 2018.

[31] Y. Shui, L. Dong, Y. Zhang, and C. Sun, "Event-based adaptive fuzzy tracking control for nonlinear systems with input magnitude and rate saturations," *Int. J. Syst. Sci.*, vol. 54, no. 16, pp. 3045–3058, Dec. 2023.

[32] J. Song, Z. Wang, Y. Niu, X. Yi, and Q.-L. Han, "Co-design of dissipative deconvolution filter and round-robin protocol for networked 2-D digital systems: Optimization and application," *IEEE Trans. Syst., Man, Cybern., Syst.*, vol. 53, no. 10, pp. 6316–6328, Oct. 2023.

[33] Y. Tan, Y. Yuan, X. Xie, E. Tian, and J. Liu, "Observer-based event-triggered control for interval type-2 fuzzy networked system with network attacks," *IEEE Trans. Fuzzy Syst.*, vol. 31, no. 8, pp. 2788–2798, Aug. 2023.

[34] E. S. Tognetti and T. M. Linhares, "Local dynamic output feedback control of saturated discrete-time T–S fuzzy systems with partially measured premise variables," *Int. J. Syst. Sci.*, vol. 54, no. 14, pp. 2784–2798, Aug. 2023.
[35] C. Wang, Z. Wang, L. Ma, H. Dong, and W. Sheng, "Subdomain-alignment data augmentation for pipeline fault diagnosis: An adversarial self-attention network," *IEEE Trans. Ind. Informat.*, vol. 20, no. 2, pp. 1374–1384, Feb. 2024.
[36] C. Wang, Z. Wang, Q. Liu, H. Dong, and W. Sheng, "Support-sample-assisted domain generalization via attacks and defenses: Concepts, algorithms, and applications to pipeline fault diagnosis," *IEEE Trans. Ind. Informat.*, vol. 20, no. 4, pp. 6413–6423, Apr. 2024.
[37] J. Wang, Y. Gao, Z. Feng, G. Sun, J. Liu, and L. Wu, "Asynchronous sliding mode control under round-robin protocol-based event-triggered communication," *IEEE Trans. Control Netw. Syst.*, vol. 10, no. 3, pp. 1424–1435, Sep. 2023.
[38] Y. Wang, H.-J. Liu, and H.-L. Tan, "An overview of filtering for sampled-data systems under communication constraints," *Int. J. Netw. Dyn. Intell.*, vol. 2, no. 3, Sep. 2023, Art. no. 100011.
[39] Y. Wang, W. Liu, C. Wang, F. Fadzil, S. Lauria, and X. Liu, "A novel multi-objective optimization approach with flexible operation planning strategy for truck scheduling," *Int. J. Netw. Dyn. Intell.*, vol. 2, no. 2, Jun. 2023, Art. no. 100002.
[40] Y. Wang, Y. Xia, C. K. Ahn, and Y. Zhu, "Exponential stabilization of Takagi–Sugeno fuzzy systems with aperiodic sampling: An aperiodic adaptive event-triggered method," *IEEE Trans. Syst., Man, Cybern., Syst.*, vol. 49, no. 2, pp. 444–454, Feb. 2019.
[41] B. Wu, X.-H. Chang, and X. Zhao, "Fuzzy H_∞ output feedback control for nonlinear NCSs with quantization and stochastic communication protocol," *IEEE Trans. Fuzzy Syst.*, vol. 29, no. 9, pp. 2623–2634, Sep. 2021.
[42] J.-W. Xing, C. Peng, Z. Cao, and W.-B. Xie, "Security-based control for networked interval type-2 fuzzy systems with multiple cyber-attacks: An improved dynamic event-triggered scheme," *IEEE Trans. Fuzzy Syst.*, vol. 31, no. 8, pp. 2747–2760, Aug. 2023.
[43] S. Yan, Z. Gu, L. Ding, J. H. Park, and X. Xie, "Weighted memory H_∞ stabilization of time-varying delayed Takagi–Sugeno fuzzy systems," *IEEE Trans. Fuzzy Syst.*, vol. 32, no. 1, pp. 337–342, Jan. 2024.
[44] Y. Zeng, H. K. Lam, B. Xiao, and L. Wu, "Tracking control for nonlinear systems with actuator saturation via interval type-2 T-S fuzzy framework," *IEEE Trans. Cybern.*, vol. 53, no. 11, pp. 7085–7094, Nov. 2023.
[45] H. Zhang, D. Yue, C. Dou, X. Xie, K. Li, and G. P. Hancke, "Resilient optimal defensive strategy of TSK fuzzy-model-based microgrids' system via a novel reinforcement learning approach," *IEEE Trans. Neural Netw. Learn. Syst.*, vol. 34, no. 4, pp. 1921–1931, Apr. 2023.
[46] L. Zhang, H.-K. Lam, Y. Sun, and H. Liang, "Fault detection for fuzzy semi-Markov jump systems based on interval type-2 fuzzy approach," *IEEE Trans. Fuzzy Syst.*, vol. 28, no. 10, pp. 2375–2388, Oct. 2020.
[47] L. Zhang, Y. Sun, H.-K. Lam, H. Li, J. Wang, and D. Hou, "Guaranteed cost control for interval type-2 fuzzy semi-Markov switching systems within a finite-time interval," *IEEE Trans. Fuzzy Syst.*, vol. 30, no. 7, pp. 2583–2594, Jul. 2022.
[48] Z. Zhang and J. Dong, "A novel H_∞ control for T–S fuzzy systems with membership functions online optimization learning," *IEEE Trans. Fuzzy Syst.*, vol. 30, no. 4, pp. 1129–1138, Apr. 2022.
[49] Z. Zhang and J. Dong, "Robust output-feedback H_∞ online optimization control for T–S fuzzy systems via differential evolution algorithm," *IEEE Trans. Fuzzy Syst.*, vol. 31, no. 11, pp. 4109–4120, Nov. 2023.
[50] H. Zhou, H.-K. Lam, B. Xiao, and C. Xuan, "Integrated fault-tolerant control design with sampled-output measurements for interval type-2 Takagi–Sugeno fuzzy systems," *IEEE Trans. Cybern.*, vol. 54, no. 9, pp. 5068–5077, Sep. 2024.
[51] Y. Xu, J. Sun, Y.-J. Pan, and Z.-G. Wu, "Optimal tracking control of heterogeneous MASs using event-driven adaptive observer and reinforcement learning," *IEEE Trans. Neural Netw. Learn. Syst.*, vol. 35, no. 4, pp. 5577–5587, Apr. 2024.

Wei Qian (Senior Member, IEEE) received the M.S. degree in control theory and control engineering from Southeast University, Nanjing, China, in 2005, and the Ph.D. degree in control science and engineering from the State Key Laboratory of Industrial Control Technology, Zhejiang University, Hangzhou, China, in 2009.

He is currently a Professor with the School of Electrical Engineering and Automation, Henan Polytechnic University, Jiaozuo, China. His current research interests include time-delay systems, nonlinear systems, networked control systems, and multiagent system.

Yanmin Wu received the B.S. degree in automation from Anyang Institute of Technology, Anyang, China, in 2019, and the M.S. degree in control theory and control engineering from Bohai University, Jinzhou, China, in 2022. He is currently pursuing the Ph.D. degree in control science and engineering with Henan Polytechnic University, Jiaozuo, China.

His current research interests include fuzzy control, event-triggered control, and security control.

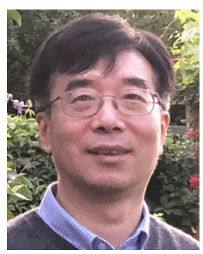

Zidong Wang (Fellow, IEEE) received the B.Sc. degree in mathematics from Suzhou University, Suzhou, China, in 1986, and the M.Sc. degree in applied mathematics and the Ph.D. degree in electrical engineering from Nanjing University of Science and Technology, Nanjing, China, in 1990 and 1994, respectively.

From 1990 to 2002, he held teaching and research appointments in universities in China, Germany, and U.K. He is currently a Professor of dynamical systems and computing with the Department of Computer Science, Brunel University London, Uxbridge, U.K. He has published a number of articles in international journals. He is a holder of the Alexander von Humboldt Research Fellowship of Germany, the JSPS Research Fellowship of Japan, and the William Mong Visiting Research Fellowship of Hong Kong. His research interests include dynamical systems, signal processing, bioinformatics, control theory, and applications.

Prof. Wang is a member of the Academia Europaea, European Academy of Sciences and Arts, and program committee for many international conferences, an Academician of the International Academy for Systems and Cybernetic Sciences, and a fellow of the Royal Statistical Society. He serves (or has served) as the Editor-in-Chief for *International Journal of Systems Science*, *Neurocomputing*, and *Systems Science and Control Engineering*, and an Associate Editor for 12 international journals, including IEEE TRANSACTIONS ON AUTOMATIC CONTROL, IEEE TRANSACTIONS ON CONTROL SYSTEMS TECHNOLOGY, IEEE TRANSACTIONS ON NEURAL NETWORKS AND LEARNING SYSTEMS, IEEE TRANSACTIONS ON SIGNAL PROCESSING, and IEEE TRANSACTIONS ON SYSTEMS, MAN, AND CYBERNETICS—PART C.